Learning to Compile Programs to Neural Networks

Logan Weber [1] Jesse Michel [1] Alex Renda [1] Michael Carbin [1]

Abstract

A *neural surrogate* is a neural network that mimics the behavior of a program. Neural surrogates of programs have been used to automatically tune program inputs, adapt programs to new settings, and accelerate computations. Neural surrogates have traditionally been developed by training on input-output examples for a single program. Language models present another approach wherein a model is trained on a single, large dataset then directly consumes program text, to act as a neural surrogate of the program. Having the language model as both the neural surrogate generator and the neural surrogate, however, poses a tradeoff of limited accuracy or excessive resource consumption. We present *neural surrogate compilation*, a technique for producing neural surrogates directly from program text without coupling neural surrogate generation and execution. We implement neural surrogate compilers using hypernetworks trained on a dataset of C programs and find they produce neural surrogates that are 1.91-$9.50\times$ as data-efficient and train in 4.31-$7.28\times$ fewer epochs than neural surrogates trained from scratch.

1. Introduction

A *neural surrogate* is a neural network that models a subset of the observable behavior of a program (Renda et al., 2021). Neural surrogates have been used to automatically configure image signal processing units and CPU simulators (Tseng et al., 2019; Renda et al., 2020), improve the accuracy of manufacturing and physics simulations (Tercan et al., 2018; Kustowski et al., 2020), accelerate the computer architecture design process (İpek et al., 2006), and accelerate computations in signal processing, robotics, 3D games, compression, machine learning, and image processing (Esmaeilzadeh et al., 2012a).

[1]MIT CSAIL, Cambridge, MA. Correspondence to: Logan Weber <loganweb@mit.edu>.

Proceedings of the 41st International Conference on Machine Learning, Vienna, Austria. PMLR 235, 2024. Copyright 2024 by the author(s).

Neural Surrogate Training. The research community has developed a variety of techniques to train neural surrogates. The traditional approach is to train a neural surrogate for a single program by collecting and curating a dataset of input-output pairs and then training a neural network to predict the program's output given an input (Renda et al., 2021).

Another point in the spectrum is to amortize the cost of training neural surrogates by training a *universal neural surrogate*: a neural network that directly consumes the text of a program and predicts the program's output for a given input (Zaremba & Sutskever, 2015; Nye et al., 2021; Gu et al., 2024). A key benefit of universal neural surrogates, compared to standard neural surrogates is that creating this dataset need only be done once, thereby enabling the creation of a neural surrogate for a given program without the need to curate a dataset of program-specific, input-output pairs.

However, universal neural surrogates necessarily use the same model to process the program text as is used to predict the program output, and accurate prediction may require multiple forward passes (e.g., chain-of-thought reasoning) (Nye et al., 2021; Wei et al., 2022). These limitations pose challenges for successfully using such a model as a neural surrogate because small models may not be able to emulate complex programs (Zaremba & Sutskever, 2015) and large models (OpenAI et al., 2023) may not be able to execute in the resource-constrained environments where neural surrogates have been used (Esmaeilzadeh et al., 2012a; Mendis, 2020; Munk et al., 2022).

Our Approach: Neural Surrogate Compilation. To maintain the benefits of universal neural surrogates while bypassing the above limitations, we propose a *neural surrogate compiler*. A neural surrogate compiler is a system that is specialized to a family of neural surrogate architectures to accept a program's text as input and produce an initial neural surrogate of the program. This initial neural surrogate can vary in behavioral quality, ranging from closely matching the behavior of the input program to only approximating the behavior of the program on a few inputs. Similarly to a traditional compiler, a neural surrogate compiler requires a significant upfront cost that is amortized over the generation of initializations for many neural surrogates. We demonstrate in this work that when

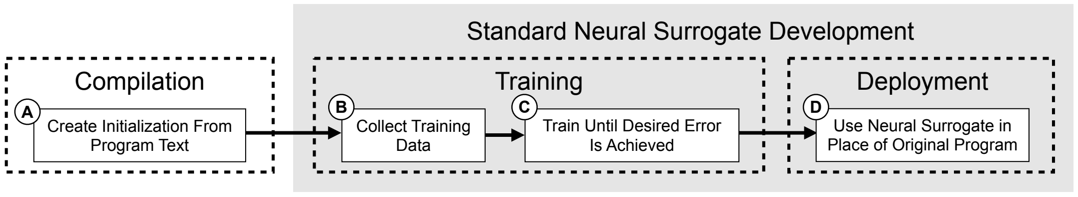
Standard Neural Surrogate Development
Compilation
A
Create Initialization From Program Text
Training
B
Collect Training Data
C
Train Until Desired Error Is Achieved
Deployment
D
Use Neural Surrogate in Place of Original Program

Figure 1: Neural surrogate development with neural surrogate compilation

compared to the traditional approach of training a neural surrogate from a random initialization, neural surrogates produced by neural surrogate compilers can be finetuned to closely mimic the behavior of the program at a lower cost—as measured in both data efficiency and training time.

Contributions. To implement a neural surrogate compiler, we adapt the BERT architecture (Turc et al., 2019) into a *hypernetwork*. A hypernetwork is a neural network that produces the parameters of another neural network (Ha et al., 2017). We name the resulting architecture COMPNET.

To train neural surrogate compilers, we develop EXESTACK, a dataset of 69,083 executable C programs collected from The Stack (Kocetkov et al., 2022), a large corpus of source code. To train COMPNETs, we refine EXESTACK into EXESTACKCPN, a dataset of 37,772 programs that is compatible with our chosen hypernetwork architecture. We then evaluate neural surrogates initialized via COMPNET on EXESTACKCPN and PARROTBENCHSHORT, the latter being a set of benchmarks from prior work in approximate computing (Esmaeilzadeh et al., 2012a).

Surrogates trained from COMPNET initializations achieve 1.91-$9.50\times$ lower error than neural surrogates trained from scratch, with the same amount of data; on a color quantization task, they produce images that are 1.02-$1.32\times$ more similar to images produced by an exact implementation than images produced by surrogates trained from random initialization; and they achieve a target error with 4.31-$7.28\times$ fewer epochs than neural surrogates trained from scratch.

2. Neural Surrogate Compilation

A *neural surrogate compiler* is a system that is specialized to a family of neural surrogate architectures to accept a program's text as input and produce an initial neural surrogate of the program. The typical strategy to train a neural surrogate is through supervised learning of a neural network with curated dataset of input-output pairs of the program (Renda et al., 2021).

In this section, we formalize the problem of efficiently training a neural surrogate and introduce a new approach to solving this problem using a *neural surrogate compiler*.

2.1. The Efficient Surrogate Training Problem

We first formalize the problem of training a neural surrogate. We assume we are given a program text $p : \mathcal{P}$ that denotes a function $[\![p]\!] : \mathcal{I}_p \to \mathcal{O}_p$,[1] where $\mathcal{I}_p$ is the type of values p accepts as input and $\mathcal{O}_p$ is the type of values p produces as output. We also assume a target neural surrogate architecture description $a : \mathcal{A}$, where $\mathcal{A} = \mathbb{R}^d \to \mathcal{I}_p \to \mathcal{O}_p$ is the space of neural network architectures, which takes a set of parameters $\theta : \mathbb{R}^d$ and produces a surrogate function from $\mathcal{I}_p$ to $\mathcal{O}_p$. The goal is to find a set of parameters $\theta : \mathbb{R}^d$ such that the neural surrogate $f : \mathcal{I}_p \to \mathcal{O}_p$ defined by $f(i) = a(\theta)(i)$ has low approximation error:

$$\forall i : \mathcal{I}_p.\, f(i) \approx [\![p]\!](i)$$

To measure the quality of a surrogate we use a loss function $\ell : \mathcal{O}_p \times \mathcal{O}_p \to \mathbb{R}^{\geq}$ that measures the difference between the output of the program and the output of the surrogate. We measure the expected loss over a distribution of inputs:

$$\mathcal{L}(f, p) = \mathbb{E}_{i \sim \mathcal{I}_p}[\ell(f(i), [\![p]\!](i))] \tag{1}$$

As with most learning problems, a challenge in training neural surrogates is that the error of a surrogate depends on the budget dedicated to collecting training data (input-output pairs of the program) and the number of epochs used to train the surrogate. We formalize these costs by defining a *training procedure* $t_a : \mathcal{P} \times \mathbb{R}^{\geq} \times \mathbb{N}^{\geq} \to \mathbb{R}^d$ for a given surrogate architecture a as a random function that takes program text p, a training data budget $b : \mathcal{R}^{\geq}$, and training time budget $n : \mathcal{R}^{\geq}$ and produces a set of parameters $\theta : \mathbb{R}^d$ for the surrogate.

We then define the *efficient surrogate training problem* as, for a given program p, architecture a, sample budget b, training time budget n, and loss function ℓ, finding a training procedure t_a that minimizes the expected loss of the resulting surrogate:

$$\arg\min_{t_a} \mathbb{E}_{\theta \sim t_a(p,b,n)}[\mathcal{L}(a(\theta), p)],$$

where $\mathcal{L}$ denotes the expected loss in Equation 1. The standard approach to training a neural surrogate is to

[1] $[\![\cdot]\!] : \mathcal{P} \to (\mathcal{I}_p \to \mathcal{O}_p)$ is notation used in programming language theory to refer to the function a program implements.

randomly initialize the parameters of the surrogate and then use a gradient-based optimization algorithm to minimize the loss against a dataset of input-output pairs of the program (Renda et al., 2021).

2.2. Neural Surrogate Compilation

A neural surrogate compiler is a system $\phi : (p : \mathcal{P}) \to \mathbb{R}^{d_p}$ that accepts program text p and produces neural network parameters $\theta \in \mathbb{R}^{d_p}$ for an architecture description a_p depending on the program p.

We use a neural surrogate compiler to solve the efficient surrogate training problem. Figure 1 presents the neural surrogate compilation workflow alongside the traditional workflow for developing a neural surrogate. In a traditional neural surrogate development workflow, one collects training data (Ⓑ), trains the neural surrogate until its error meets the desired threshold (Ⓒ), and then uses it in place of the original program (Ⓓ). Neural surrogate compilation (Ⓐ) introduces a new, initial step in the neural surrogate compilation workflow in which a neural surrogate compiler maps the program text to a neural network initialization for use in the training of the neural surrogate.

We formalize the development of a neural surrogate compiler as an optimization problem. The goal is to develop a ϕ such that for every program p, the surrogate $f = a_p(\phi(p))$ can be trained efficiently. Optimizing for a system that generates surrogates that can be trained efficiently is challenging. As a simple proxy, we optimize for a system that generates surrogates that achieve low loss:

$$\underset{\phi \in \mathcal{P} \to \mathbb{R}^d}{\arg\min}\ \mathbb{E}_{p \sim \mathcal{P}}[\mathcal{L}(a_p(\phi(p)), p)].$$

3. COMPNET

A COMPNET is an implementation of a neural surrogate compiler using hypernetworks. We explain the COMPNET architecture, how to train them, then how to extract neural surrogates from their outputs.

3.1. Architecture

Figure 2 presents the design of a COMPNET. A COMPNET accepts program text as input and produces parameters for a neural surrogate architecture $a : \mathbb{R}^d \to \mathcal{I} \to \mathcal{O}$ with as many inputs as the largest architecture one wishes to compile to (e.g., an architecture with 9 inputs can be used to compile functions with at most 9 inputs) and a single output. We call this architecture a *covering architecture*.

Ⓐ First, COMPNET tokenizes an input program ($\boxed{1}$), resulting in a sequence of tokens ($\boxed{2}$) including the distinguished BERT *classification token* `[CLS]`.

Ⓑ COMPNET then uses a BERT encoder (Devlin et al., 2019) to embed the sequence of tokens, resulting in an embedding per token. The output of this step is the embedding of the classification token ($\boxed{3}$); COMPNET discards the embeddings of the other tokens.

Ⓒ Next, COMPNET uses a linear layer to map the classification token embedding to a neural surrogate parameter vector ($\boxed{4}$).

Ⓓ Then, COMPNET interprets the vector of neural surrogate parameters as the weights and biases of the covering architecture. The output of this step is a neural surrogate of the input program.

Ⓔ Finally, COMPNET executes the neural surrogate with the interpreted parameters on a program input ($\boxed{5}$) to produce a prediction of the program output ($\boxed{6}$).

3.2. Training

Training a COMPNET requires a dataset of programs and input-output pairs for each program. Note that this dataset is not considered as part of the budget in the efficient surrogate training problem, since it is amortized over all programs the COMPNET is used to compile.

Each step of training proceeds by selecting a batch of programs and input-output pairs for those programs, generating neural surrogate parameters for each program, interpreting the neural surrogate parameters as parameters for the covering architecture, executing each neural surrogate with the batch of inputs, then calculating the loss between the neural surrogates' predicted outputs and the true outputs. To match the signature of the covering architecture, the batch of inputs is padded out to match the number of inputs for the covering architecture. For padding, we use inputs drawn from the same distribution as the program inputs (see Appendix N for details).

Backpropagation proceeds as usual, except that one does not update the parameters of the neural surrogates, since each generated neural surrogate is ephemeral. Instead, backpropgation only updates the parameters of the COMPNET. Appendix G presents additional training details.

3.3. Surrogate Extraction

The output of a COMPNET is parameters for the covering architecture, which might not match the number of inputs and outputs of the program being compiled. To adapt the covering architecture to the target number of inputs, one finetunes the resulting architecture on data where the excess inputs are set to zero, allowing one to then remove the weights in the input layer corresponding to the excess inputs (see Appendix N for details on this choice). To adapt the covering architecture to the target number of outputs, one

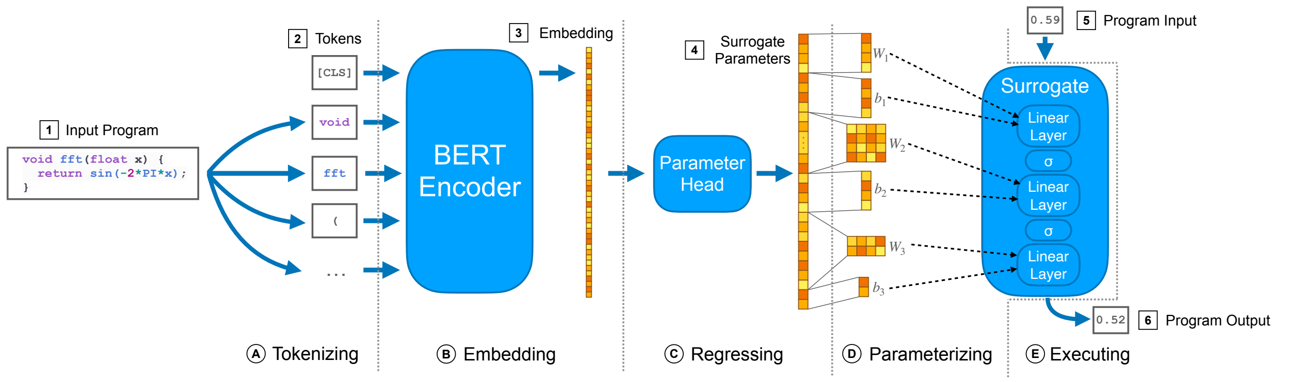

Figure 2: System diagram describing the COMPNET architecture, comprising five phases: (A) tokenizing an input program, (B) embedding the program using a BERT, (C) regressing the embeddings to a parameter weight vector using a parameter head, (D) parameterizing a neural network using the parameter weight vector, and (E) executing the neural network surrogate.

clones the weights for the single output in the output layer for each new output that is needed (see Appendix O for details on this choice). When neither the number of inputs nor the number of outputs matches the target, both of the above modifications are applied in the same finetuning run.

4. EXESTACK

The strategy we presented in Section 3 for learning a neural surrogate compiler requires a dataset of programs and input-output examples describing the behavior of each program. To fulfill this requirement, we developed EXESTACK, a dataset of numerical, executable, deterministic C programs and corresponding input-output examples. EXESTACK is based on The Stack, a dataset of 3 TB of permissively licensed source code written in various programming languages scraped from GitHub (Kocetkov et al., 2022).

Figure 3 summarizes the process by which we produced a dataset of 69,083 pointer-free, numerical, executable, deterministic C programs, along with a set of input-output examples for each program. We provide a detailed description of each step of the process in Appendix B. We note that the restriction to pointer-free functions simplifies the EXESTACK generation methodology. However, a model trained on EXESTACK could still handle programs using statically-sized data structures containing numeric data (e.g., arrays), as they can be transformed into functions with a fixed number of arguments.

5. Evaluation

To evaluate the claim that neural surrogate compilation lowers the development cost of neural surrogates, we answer the following research questions.

RQ 1: Does a neural surrogate initialized by a COMPNET converge to a lower test loss than a neural surrogate initialized randomly, for a fixed training set size?

RQ 2: Does a neural surrogate initialized by a COMPNET produce better perceptual results in an end-to-end application than a neural surrogate initialized randomly, for a fixed training set size?

RQ 3: Does a neural surrogate initialized by a COMPNET converge to a target test loss in fewer epochs than a neural surrogate initialized randomly?

Our results demonstrate that COMPNETs lead to improvements in data efficiency (Section 5.2), perceptual quality (Section 5.3), and training time (Appendix L).

5.1. Methodology

To develop and evaluate COMPNETs, we use a BERT architecture for the neural surrogate compiler and a multilayer perceptron for the surrogate, produce datasets COMPNETs can be trained and evaluated on, introduce alternative initialization methods to compare against, and finetune surrogates produced by initialization methods.

5.1.1. COMPNET ARCHITECTURE AND TRAINING

We use the BERT-Tiny architecture (Turc et al., 2019) for the neural surrogate compiler. As our compilation target, we adapt a neural surrogate architecture from Esmaeilzadeh et al. (2012a) into a covering architecture. The architecture in Esmaeilzadeh et al. (2012a) is a multilayer perceptron consisting of a single input, a hidden layer of 4 neurons, another hidden layer of 4 neurons, and 2 outputs, and it uses a sigmoid activation function. Esmaeilzadeh et al. (2012a) demonstrate that their techniques achieve a 3.6× speedup on their fast Fourier transform benchmark (2012a)

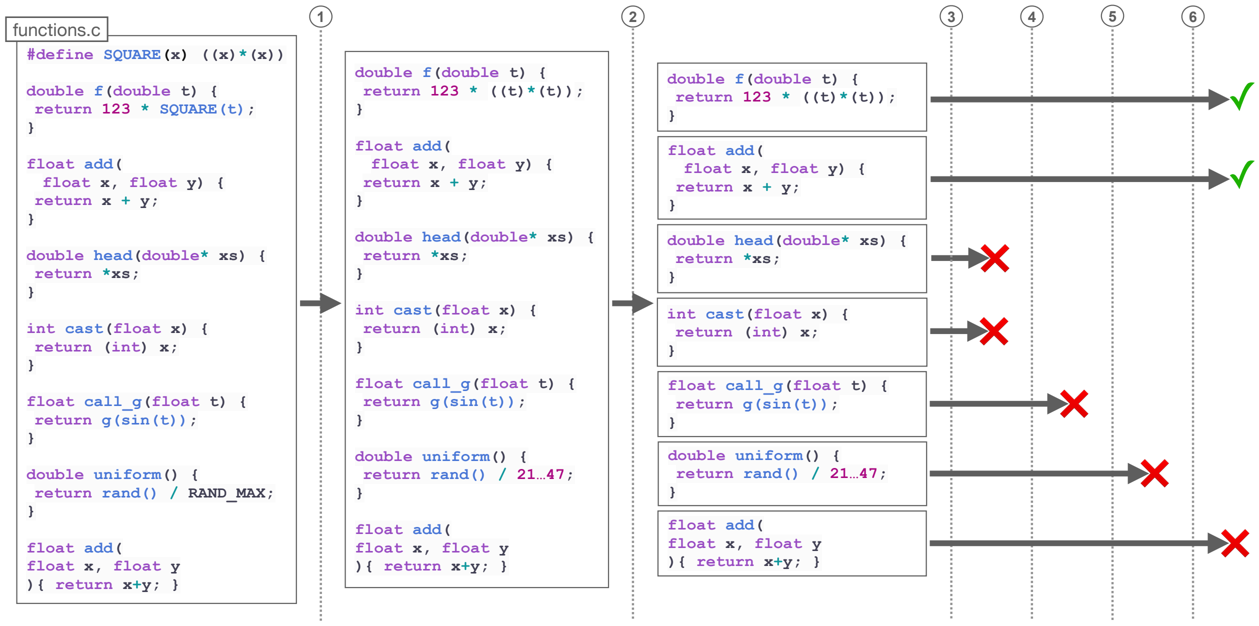

```
#define SQUARE(x) ((x)*(x))

double f(double t) {
 return 123 * SQUARE(t);
}

float add(
  float x, float y) {
 return x + y;
}

double head(double* xs) {
 return *xs;
}

int cast(float x) {
 return (int) x;
}

float call_g(float t) {
 return g(sin(t));
}

double uniform() {
 return rand() / RAND_MAX;
}

float add(
float x, float y
){ return x+y; }
```

```
double f(double t) {
 return 123 * ((t)*(t));
}

float add(
  float x, float y) {
 return x + y;
}

double head(double* xs) {
 return *xs;
}

int cast(float x) {
 return (int) x;
}

float call_g(float t) {
 return g(sin(t));
}

double uniform() {
 return rand() / 21…47;
}

float add(
float x, float y
){ return x+y; }
```

```
double f(double t) {
 return 123 * ((t)*(t));
}
```

```
float add(
  float x, float y) {
 return x + y;
}
```

```
double head(double* xs) {
 return *xs;
}
```

```
int cast(float x) {
 return (int) x;
}
```

```
float call_g(float t) {
 return g(sin(t));
}
```

```
double uniform() {
 return rand() / 21…47;
}
```

```
float add(
float x, float y
){ return x+y; }
```

Figure 3: The EXESTACK generation pipeline. Starting with C source files from The Stack, we apply a sequence of maps followed by a sequence of filters. The steps are (1) run the C preprocessor, (2) extract functions from the source file, (3) remove functions with pointers in their type signature and nonnumeric functions, (4) remove nonexecutable functions and collect input-output pairs, (5) remove nondeterministic functions, and (6) remove any duplicate programs. Red "X"s denote that a function does not pass a filter and green checkmarks denote that a function passes all filters.

Benchmark	Description	Train Inputs	Test Inputs	#Inputs	#Outputs
`fft`	Radix-2 Cooley-Tukey fast Fourier transform	32,768 random floating point numbers	2,048 random floating point numbers	1	2
`invk2j`	Inverse kinematics for 2-joint arm	10,000 random (x, y) coordinates	10,000 random (x, y) coordinates	2	2
`kmeans`	k-means clustering	50,000 random (r, g, b) values	220x200 color image	6	1
`sobel`	Sobel edge detector	One 512x512 color image	220x200 color image	9	1

Table 1: The programs from PARROTBENCH we include in PARROTBENCHSHORT (Esmaeilzadeh et al., 2012a).

relative to the original program when using this architecture. This architecture therefore places a floor on the system speedup that motivates our investigation of Parrot in that the architectures that Esmaeilzadeh et al. (2012a) use for all other programs in PARROTBENCHSHORT at least as computational expensive as the one we choose.

We adapt this architecture to take in 9 inputs and produce 1 output so it can be used to compile programs with up to 9 inputs. We additionally develop a methodology to build surrogates for programs using up to 9 inputs and arbitrarily many outputs during finetuning (see Section 3 and Appendices N and O for more details).

5.1.2. DATASETS

EXESTACKCPN is a variant of EXESTACK that we use to train COMPNETs for a chosen hypernet architecture. We evaluate the effectiveness of COMPNETs on programs from the test set of EXESTACKCPN and programs from PARROTBENCHSHORT, a subset of the suite of benchmarks introduced by Esmaeilzadeh et al. (2012a) (Table 1).

EXESTACKCPN. EXESTACKCPN contains 37,772 programs, each with 2,048 input-output examples. See Appendix E for details on EXESTACKCPN generation.

From the full set of programs, we created a train, validation, and test set using an 80/10/10 split. Each program has input-output examples, so we additionally create

Statistic	CPN	MAML	PTS
0th	$6.36 \cdot 10^{-8}\times$	$4.68 \cdot 10^{-6}\times$	$1.35 \cdot 10^{-4}\times$
25th	$1.23\times$	$0.87\times$	$0.76\times$
50th	$5.84\times$	$1.17\times$	$1.28\times$
75th	$54.36\times$	$1.71\times$	$2.66\times$
100th	$4.43 \cdot 10^{7}\times$	$8.52 \cdot 10^{3}\times$	$7.14 \cdot 10^{4}\times$
MPI	21st	35th	37th
GM	$9.50\times$	$1.09\times$	$1.08\times$

Dataset Size	CPN	MAML	PTS
0%	$84.40\times$	$1.42\times$	$2.63\times$
0.1%	$10.43\times$	$0.91\times$	$0.87\times$
1%	$2.90\times$	$0.51\times$	$0.90\times$
10%	$4.12\times$	$1.54\times$	$0.88\times$
100%	$6.67\times$	$1.53\times$	$0.76\times$

Figure 4: Geometric mean test-input loss improvement over random initialization on $1,000$ EXESTACKCPN test programs, taken over all programs and dataset sizes (left), and grouped by dataset sizes (right). The table on the left reports improvements at a sample of percentiles from 0th (performance that is the worst compared to random initialization) to 100th (performance that is the best compared to random initialization), the minimum percentile at which an initialization method improves over random initialization (MPI), and overall geometric mean improvements (GM).

Stat.	CPN	MAML	PTS
0th	$0.22\times$	$0.28\times$	$0.23\times$
25th	$0.88\times$	$0.82\times$	$0.75\times$
50th	$1.23\times$	$0.97\times$	$0.97\times$
75th	$2.96\times$	$1.14\times$	$1.26\times$
100th	$106.91\times$	$1.99\times$	$38.18\times$
MPI	36th	54th	54th
GM	$1.91\times$	$0.93\times$	$1.05\times$

Program	CPN	MAML	PTS
`fft`	$1.47\times$	$0.98\times$	$0.61\times$
`invk2j`	$1.01\times$	$1.07\times$	$1.05\times$
`kmeans`	$7.85\times$	$0.68\times$	$2.24\times$
`sobel`	$1.14\times$	$1.06\times$	$0.85\times$

% Data	CPN	MAML	PTS
0%	$1.81\times$	$0.90\times$	$1.56\times$
0.1%	$1.98\times$	$0.94\times$	$0.98\times$
1%	$1.77\times$	$0.93\times$	$0.79\times$
10%	$2.38\times$	$1.11\times$	$1.23\times$
100%	$1.68\times$	$0.81\times$	$0.86\times$

Figure 5: Geometric mean test-input loss improvement over random initialization on PARROTBENCHSHORT, taken over all programs and dataset sizes (top), grouped by programs (bottom left), and grouped by dataset sizes (bottom right). The top table reports improvements at a sample of percentiles from 0th to 100th, the minimum percentile at which an initialization method improves over random initialization (MPI), and overall geometric mean improvements (GM).

a train and test set for these examples using a 50/50 split. In Sections 5.2 and L, we evaluate performance on EXESTACKCPN using 1,000 programs from the test set.

Parrot Benchmarks. We adapt PARROTBENCHSHORT from the original benchmark suite of Esmaeilzadeh et al., which we refer to as PARROTBENCH (2012a). PARROTBENCHSHORT programs come from a diverse set of application domains, they are all written in C, each consists of a single function, and they are numeric in nature, making them suitable for evaluating COMPNETS. Table 1 shows the programs in PARROTBENCHSHORT, including descriptions of the computations and datasets. In Appendix F provide more detail on these benchmark programs.

5.1.3. ALTERNATIVE INITIALIZATION METHODS

We compare COMPNETS to two alternative techniques, neither of which conditions on program text: model-agnostic meta learning (MAML) (Finn et al., 2017) and pretrained initializations. Both techniques result in constant initializations that one uses for every program. In Appendix A, we survey related work in this area in detail. We train 3 instances of each initialization method on EXESTACKCPN training programs using the same covering architecture as COMPNETS.

Model-Agnostic Meta Learning. MAML is a meta-learning technique for producing neural network initializations that can be quickly finetuned to achieve low error on any task sampled from some space of tasks. See Appendices H, N , and O for details on training, input padding, and variable-output support, respectively.

Pretrained Neural Surrogates. A simpler alternative to MAML is to train a single neural surrogate on all input-output examples of EXESTACK, ignoring program text. We call initializations trained in this way *pretrained neural surrogates* (PTS). See Appendices I, N , and O for details.

Distinguishing Initialization Methods. For brevity, we use shorthand names for each initialization method in figures. We refer to COMPNETS as "CPN", MAML as "MAML", pretrained surrogates as "PTS", and random initialization as "RND".

5.1.4. FINETUNING SURROGATES

Here we collect methodology and discussion relevant to all surrogates we finetune in this evaluation, including optimization methods, hyperparameters, random seed behavior, and a discussion of how we measure the improvements achieved by these surrogates.

For all surrogates produced by the initialization methods we consider, we use the following methodology. We use the Adam optimizer with no weight decay, a learning rate of 0.01, and mean squared error as the loss function. The only difference between our methodology and the methodology of Esmaeilzadeh et al. (2012a) is that we use the Adam optimizer instead of stochastic gradient descent and we use the He initialization method (He et al., 2015)—they do not specify how they initialize their neural surrogates.

We use 9 trials with different random seeds for every configuration in the experiments that follow. Note that, for COMPNET, MAML, and PTS initializations, changing random seeds only changes the training data order, since the initialization is deterministic.

We primarily consider geometric mean improvements over test loss and training time in our evaluation. These are only relative measures, so in Appendix M, we the trained neural surrogates achieve sufficiently low absolute error for downstream applications.

5.2. Data Efficiency Improvements

To assess whether COMPNETs improve data efficiency, we use COMPNETs to initialize neural surrogates, finetune on subsets of training data of various sizes, and then compare the results to those of other initialization methods. We detail the methodology of this experiment then present results.

5.2.1. METHODOLOGY

We now describe the configurations we sweep over and the methodology we use to finetune surrogates.

Experiment Configurations. In this experiment, we sweep over configurations consisting of a program, a dataset size, and an initialization method (e.g., a COMPNET). Each dataset size specifies the percentage of the training data to train neural surrogates on. We sweep over the following percentages: $\{0\%, 0.1\%, 1\%, 10\%, 100\%\}$.

Dataset Selection. Given a configuration consisting of a program, dataset size percentage c, and an initialization method, we select a random subset $\mathcal{D}_{\text{sub}}$ of the training data $\mathcal{D}_{\text{train}}$ of size $c|\mathcal{D}_{\text{train}}|$. We use an $80/20$ split to divide $\mathcal{D}_{\text{sub}}$ into train and validation sets $\mathcal{D}_{\text{sub train}}$ and $\mathcal{D}_{\text{sub val}}$. We sample 9 different subsets of this size and use a different training seed for each subset, yielding 9 trials total.

Finetuning. For each trial, we initialize a neural surrogate according to the initialization method. We then train on $\mathcal{D}_{\text{sub train}}$ for $5{,}000$ epochs. The final test loss we report for a trial is the test loss at the epoch closest to the epoch with the lowest validation error.[2] When the dataset size is 0%, we use the test loss at the final epoch.

Quantifying Improvements. We define the improvement for a given configuration (consisting of an initialization method, program, and dataset size) as the ratio of the test loss achieved by random initialization on that configuration and the test loss achieved by that configuration. All test losses are averaged over trials (using arithmetic mean) prior to computing ratios. For each initialization method, we report the geometric mean of the improvements grouped by program, grouped by dataset size, and overall. For some programs and initialization methods, the resulting surrogates achieve losses of 0. We discard these results before computing the geometric mean.

These are only relative measures, so in Appendix M, we demonstrate that the neural surrogates we train achieve sufficiently low absolute error for downstream applications.

5.2.2. RESULTS

Figures 4 and 5 show finetuning results for a sample of 1,000 EXESTACKCPN test programs and PARROTBENCHSHORT, respectively. See Appendix J for details.

EXESTACKCPN Test Programs. COMPNETs achieve the best results on average, with a $9.50\times$ improvement over random initialization, whereas MAML and pretrained surrogates achieve only a $1.09\times$ and $1.08\times$ improvement on average. COMPNETs improve over random initialization in as low as the 21st percentile of configurations, whereas MAML and pretrained surrogates improve over random initialization after the 35th and 37th percentiles, respectively.

COMPNETs improve on EXESTACKCPN test programs most prominently in the zero-shot regime, where the improvement is $84.40\times$ over random initialization, whereas MAML and pretrained surrogates achieve improvements of $1.42\times$ and $2.63\times$, respectively. The zero-shot regime is also the only regime where pretrained surrogates show an improvement. The worst performance for both COMPNETs and MAML is in the middle of the dataset sizes we evaluated, at a dataset size of 1%, where they achieved $2.90\times$ and $0.51\times$, respectively. The worst performance for pretrained surrogates, however, is at a dataset size of 100%.

PARROTBENCHSHORT Programs. COMPNETs achieve the best results on average, achieving a $1.91\times$ improvement over random initialization, whereas MAML worsened performance ($0.93\times$) and pretrained surrogates slightly improved performance ($1.05\times$). COMPNETs improve over random initialization in as low as the 36th

[2]We only compute test loss before training, after every 3 epochs of training, and after training.

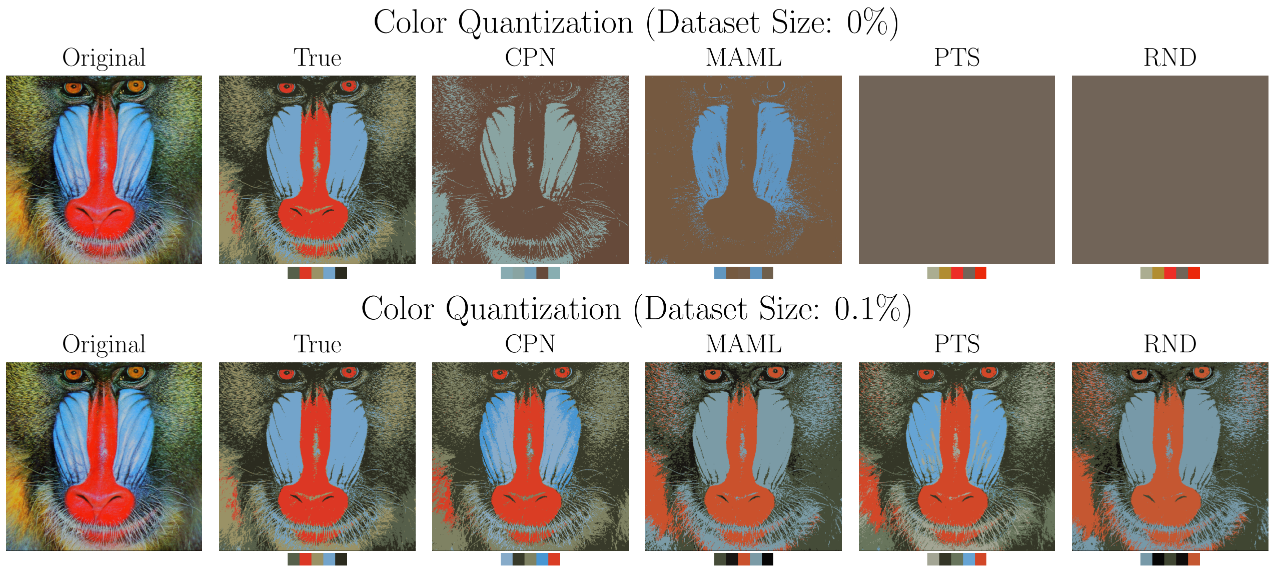
Color Quantization (Dataset Size: 0%)
Original
True
CPN
MAML
PTS
RND
Color Quantization (Dataset Size: 0.1%)
Original
True
CPN
MAML
PTS
RND

Figure 6: Color quantization results for a ground-truth implementation ("True") vs. approximate implementations. The original image of a baboon is on the left, followed by images transformed to adhere to a palette of 5 colors.

percentile of configurations, whereas MAML and pretrained surrogates both improve over random initialization after the 54th percentile, respectively.

CompNets improve or do not worsen data efficiency on each ParrotBenchShort program, with the smallest improvement on `invk2j` ($1.01\times$) and the largest improvement on `kmeans` ($7.85\times$). MAML shows the largest improvement on `invk2j` ($1.07\times$) but worsens performance on `fft` and `kmeans`, achieving $0.98\times$ and $0.68\times$, respectively. Pretrained surrogates show the largest improvement on `kmeans` ($2.24\times$), but they worsen performance on `fft` and `sobel`, achieving $0.61\times$ and $0.85\times$, respectively.

Unlike the results for ExeStackCPN, the improvement due to CompNets is most pronounced near the middle of the dataset sizes we evaluated over. The greatest improvement of $2.38\times$ occurs at 10%, and the smallest improvement of $1.68\times$ occurs at 100%. MAML worsens performance at most dataset sizes, except at 10%, where it achieves a $1.11\times$ improvement over random initialization. Pretrained surrogates worsen performance at most dataset sizes except 0% and 10%, where they achieve $1.56\times$ and $1.23\times$, respectively.

Since CompNets improve data efficiency over random initialization on both ExeStackCPN and ParrotBenchShort, we answer yes to RQ 1.

5.3. Neural Surrogates for Color Quantization

To assess whether a CompNet can improve the quality of results in an end-to-end application, we use a CompNet to initialize a neural surrogate used for *color quantization* and compare it to other initialization methods (Kanungo et al., 2002). Color quantization is the process of reducing the number of distinct colors in an image.

5.3.1. Methodology

We present the methodology for an end-to-end evaluation of neural surrogates on color quantization. We follow the methodology of Kanungo et al. (2002) who apply k-means clustering to the (R, G, B) vectors representing the colors of pixels of an image and select the cluster centroids as the colors in the palette. We run k-means clustering for 40 iterations or until the distance between the old centroids and new centroids is less than $1 \cdot 10^{-5}$. Each pixel color is then remapped to the closest color in the palette.

We use the Euclidean distance function to compute the distance between two RGB vectors. We consider both a standard implementation and approximate implementations given by neural surrogates of the `kmeans` kernel in ParrotBenchShort. We use the surrogates from the data efficiency evaluation of Section 5.2.

5.3.2. Results

Figure 6 depicts the result of applying color quantization to an image of a baboon. The original image is on the left, followed by images quantized to a palette of 5 colors. The "True" quantization uses a standard implementation of the Euclidean distance function and the subsequent images use the different surrogate initialization methods: CPN, MAML, PTS, and RND. The surrogate models used to produce these images are from the data efficiency evaluation (Section 5.2)

Dataset Size	CPN	MAML	PTS	RND
0%	$2.67 \cdot 10^3 \pm 541.$	$2.79 \cdot 10^3 \pm 347.$	$3.04 \cdot 10^3 \pm 63.0$	$3.05 \cdot 10^3 \pm 0.00$
0.1%	$984.0 \pm 733.$	$1.79 \cdot 10^3 \pm 554.$	$1.73 \cdot 10^3 \pm 725.$	$1.43 \cdot 10^3 \pm 544.$
1%	$528. \pm 219.$	$782. \pm 300.$	$760. \pm 256.$	$619. \pm 249.$
10%	$452. \pm 222.$	$717. \pm 212.$	$690. \pm 195.$	$782. \pm 307.$
100%	$504. \pm 220.$	$766. \pm 189.$	$699. \pm 171.$	$655. \pm 121.$

Dataset Size	CPN	MAML	PTS	RND
0%	0.33 ± 0.11	0.26 ± 0.03	0.25 ± 0.02	0.25 ± 0.0
0.1%	0.61 ± 0.15	0.45 ± 0.12	0.47 ± 0.16	0.53 ± 0.09
1%	0.72 ± 0.12	0.64 ± 0.11	0.65 ± 0.10	0.70 ± 0.11
10%	0.76 ± 0.12	0.64 ± 0.09	0.64 ± 0.08	0.63 ± 0.08
100%	0.73 ± 0.13	0.62 ± 0.08	0.64 ± 0.05	0.65 ± 0.06

Figure 7: Quantitative comparison of end-to-end results produced by various initialization methods on color quantization with a palette size of 5 colors. **(Top)** The average mean squared error (MSE) of the image produced by each initialization method compared to the image produced by a ground-truth implementation of the `kmeans` kernel (lower is better). **(Bottom)** The average structural similarity index measure (SSIM) of the image produced by each initialization method compared to the image produced by a ground-truth implementation of the `kmeans` kernel (higher is better).

with dataset sizes of 0% and 0.1%. For each initialization method, there are many surrogates to choose from. For the surrogates trained on a dataset size of 0%, we use the full train set from PARROTBENCHSHORT as a validation set and choose the surrogate with the lowest validation loss. For the surrogates trained on a dataset size of 0.1%, we use the dataset it was trained on, as in Section 5.2.

Figure 7 shows quantitative results comparing initialization methods on 5-color color quantization at various dataset sizes. See Appendix K for more color palette sizes. We use all surrogates from the data efficiency evaluation. Each entry shows the average and standard deviation of a metric over all trials and instances of an initialization method.

The first table depicts the mean squared error (MSE) that sweeps across dataset sizes for each initialization method. Among the initialization methods, CPN has the lowest (best) mean MSE across runs for every dataset size. The results for MAML, PTS, and RND with no clear best method among them. The variance is similar across all initialization methods, and is high enough that there is overlap among methods. For example, at 0% dataset size a result that is one standard deviation below the mean for MAML is lower than the mean for CPN. However, for all other dataset sizes the mean MSE for CPN is lower than the mean MSE for MAML even after subtracting a single standard deviation.

The second table depicts the structural similarity index measure (SSIM), which provides a quantitative model for the percieved similarity of images (Wang et al., 2004). Among the initialization methods, CPN has the highest (best) mean SSIM across runs for every dataset size. The results for MAML, PTS, and RND are similar to the MSE results, but RND is performs slightly better than either MAML or PTS at most dataset sizes. At smaller dataset sizes, the variance is high enough that there is overlap among methods, but at larger dataset sizes the results are more clearly separated with CPN having the highest mean SSIM even when we consider adding a single standard deviation to the mean SSIM for each of the other initialization methods.

6. Conclusion

In this paper, we presented the concept of a neural surrogate compiler and demonstrated how a neural surrogate compiler can be implemented with COMPNETS. We provided a dataset, EXESTACK, that one can use to learn neural surrogate compilers. We demonstrated the effectiveness of COMPNETS on EXESTACK programs and PARROTBENCHSHORT, a suite of numerical benchmarks. Specifically, we showed COMPNET-initialized surrogates achieve losses 1.91-$9.50\times$ lower than randomly initialized surrogates, produce color-quantized images that are 1.02-$1.32\times$ more similar to images produced by an exact implementation than images produced by randomly initialized surrogates, and train in 4.31-$7.28\times$ fewer epochs than randomly initialized surrogates.

The key insight of our work is a programming language can condition the space of neural network initializations. In the limit, a neural surrogate compiler could produce initializations requiring no training to achieve low error. More broadly, neural surrogate compilers could be used to encode programmatically specified behaviors in neural networks, potentially accelerating training for more general tasks.

Impact Statement

This paper presents work whose goal is to advance the field of Machine Learning. There are many potential societal consequences of our work, none of which we feel must be specifically highlighted here.

Acknowledgements

We would like to thank Ellie Cheng, Charles Yuan, and the anonymous reviewers for their helpful comments and suggestions. This work was supported in-part by the National Science Foundation (CCF-1918839 and CCF-2217064) and an Intel Research Fellowship.

References

An, S., Fowler, C., Zheng, B., Shalaginov, M. Y., Tang, H., Li, H., Zhou, L., Ding, J., Agarwal, A. M., Rivero-Baleine, C., Richardson, K. A., Gu, T., Hu, J., and Zhang, H. A deep learning approach for objective-driven all-dielectric metasurface design. *ACS Photonics*, 2019.

Austin, J., Odena, A., Nye, M., Bosma, M., Michalewski, H., Dohan, D., Jiang, E., Cai, C., Terry, M., Le, Q., and Sutton, C. Program synthesis with large language models. *arXiv preprint 2108.07732*, 2021.

Baek, W. and Chilimbi, T. M. Green: A framework for supporting energy-conscious programming using controlled approximation. In *Programming Language Design and Implementation*, 2010.

Bieber, D., Sutton, C., Larochelle, H., and Tarlow, D. Learning to execute programs with instruction pointer attention graph neural networks. In *International Conference on Neural Information Processing Systems*, 2020.

Bubeck, S., Chandrasekaran, V., Eldan, R., Gehrke, J., Horvitz, E., Kamar, E., Lee, P., Lee, Y. T., Li, Y., Lundberg, S., Nori, H., Palangi, H., Ribeiro, M. T., and Zhang, Y. Sparks of artificial general intelligence: Early experiments with gpt-4. *arXiv preprint 2303.12712*, 2023.

Devlin, J., Chang, M.-W., Lee, K., and Toutanova, K. Bert: Pre-training of deep bidirectional transformers for language understanding. In *North American Chapter of the Association for Computational Linguistics*, 2019.

Esmaeilzadeh, H., Sampson, A., Ceze, L., and Burger, D. Neural acceleration for general-purpose approximate programs. In *International Symposium on Microarchitecture*, 2012a.

Esmaeilzadeh, H., Sampson, A., Ceze, L., and Burger, D. Architecture support for disciplined approximate programming. In *International Conference on Architectural Support for Programming Languages and Operating Systems*, 2012b.

Finn, C., Abbeel, P., and Levine, S. Model-agnostic meta-learning for fast adaptation of deep networks. In *International Conference on Machine Learning*, 2017.

Gu, A., Rozière, B., Leather, H., Solar-Lezama, A., Synnaeve, G., and Wang, S. I. Cruxeval: A benchmark for code reasoning, understanding and execution. *arXiv preprint 2401.03065*, 2024.

Ha, D., Dai, A. M., and Le, Q. V. Hypernetworks. In *International Conference on Learning Representations*, 2017.

He, K., Zhang, X., Ren, S., and Sun, J. Delving deep into rectifiers: Surpassing human-level performance on imagenet classification. In *IEEE International Conference on Computer Vision*, 2015.

Hospedales, T., Antoniou, A., Micaelli, P., and Storkey, A. Meta-learning in neural networks: A survey. 44(09), 2022.

İpek, E., McKee, S. A., Caruana, R., de Supinski, B. R., and Schulz, M. Efficiently exploring architectural design spaces via predictive modeling. In *International Conference on Architectural Support for Programming Languages and Operating Systems*, 2006.

Jin, T., Liu, Z., Yan, S., Eichenberger, A., and Morency, L.-P. Language to network: Conditional parameter adaptation with natural language descriptions. In *Annual Meeting of the Association for Computational Linguistics*, 2020.

Kanungo, T., Mount, D. M., Netanyahu, N. S., Piatko, C. D., Silverman, R., and Wu, A. Y. An efficient k-means clustering algorithm: Analysis and implementation. 24, 2002.

Kaya, M. and Hajimirza, S. Using a novel transfer learning method for designing thin film solar cells with enhanced quantum efficiencies. *Scientific Reports*, 2019.

Kocetkov, D., Li, R., Ben Allal, L., Li, J., Mou, C., Muñoz Ferrandis, C., Jernite, Y., Mitchell, M., Hughes, S., Wolf, T., Bahdanau, D., von Werra, L., and de Vries, H. The stack: 3 tb of permissively licensed source code. *arXiv preprint 2211.15533*, 2022.

Kustowski, B., Gaffney, J. A., Spears, B. K., Anderson, G. J., Thiagarajan, J. J., and Anirudh, R. Transfer learning as a tool for reducing simulation bias: Application to inertial confinement fusion. *Transactions on Plasma Science*, 2020.

Kwon, J. and Carloni, L. P. Transfer learning for design-space exploration with high-level synthesis. In *Workshop on Machine Learning for CAD*, 2020.

Li, R., Allal, L. B., Zi, Y., Muennighoff, N., Kocetkov, D., Mou, C., Marone, M., Akiki, C., Li, J., Chim, J., Liu, Q., Zheltonozhskii, E., Zhuo, T. Y., Wang, T., Dehaene, O., Davaadorj, M., Lamy-Poirier, J., Monteiro, J., Shliazhko, O., Gontier, N., Meade, N., Zebaze, A., Yee, M.-H., Umapathi, L. K., Zhu, J., Lipkin, B., Oblokulov, M., Wang, Z., Murthy, R., Stillerman, J., Patel, S. S., Abulkhanov, D., Zocca, M., Dey, M., Zhang, Z., Fahmy, N., Bhattacharyya, U., Yu, W., Singh, S., Luccioni, S., Villegas, P., Kunakov, M., Zhdanov, F., Romero, M., Lee, T., Timor, N., Ding, J., Schlesinger, C., Schoelkopf, H., Ebert, J., Dao, T., Mishra, M., Gu, A., Robinson, J., Anderson, C. J., Dolan-Gavitt, B., Contractor, D., Reddy, S., Fried, D., Bahdanau, D., Jernite, Y., Ferrandis, C. M., Hughes, S., Wolf, T., Guha, A., von Werra, L., and de Vries, H. Starcoder: may the source be with you! *arXiv preprint arXiv:2305.06161*, 2022.

Lozhkov, A., Li, R., Allal, L. B., Cassano, F., Lamy-Poirier, J., Tazi, N., Tang, A., Pykhtar, D., Liu, J., Wei, Y., Liu, T., Tian, M., Kocetkov, D., Zucker, A., Belkada, Y., Wang, Z., Liu, Q., Abulkhanov, D., Paul, I., Li, Z., Li, W.-D., Risdal, M., Li, J., Zhu, J., Zhuo, T. Y., Zheltonozhskii, E., Dade, N. O. O., Yu, W., Krauß, L., Jain, N., Su, Y., He, X., Dey, M., Abati, E., Chai, Y., Muennighoff, N., Tang, X., Oblokulov, M., Akiki, C., Marone, M., Mou, C., Mishra, M., Gu, A., Hui, B., Dao, T., Zebaze, A., Dehaene, O., Patry, N., Xu, C., McAuley, J., Hu, H., Scholak, T., Paquet, S., Robinson, J., Anderson, C. J., Chapados, N., Patwary, M., Tajbakhsh, N., Jernite, Y., Ferrandis, C. M., Zhang, L., Hughes, S., Wolf, T., Guha, A., von Werra, L., and de Vries, H. Starcoder 2 and the stack v2: The next generation. *arXiv preprint 2402.19173*, 2024.

Mendis, C. *Towards Automated Construction of Compiler Optimizations*. Ph.d. thesis, Massachusetts Institute of Technology, Cambridge, MA, 2020.

Misailovic, S., Sidiroglou, S., Hoffmann, H., and Rinard, M. Quality of service profiling. In *International Conference on Software Engineering*, 2010.

Munk, A., Zwartsenberg, B., Scibior, A., Baydin, A. G., Stewart, A. L., Fernlund, G., Poursartip, A., and Wood, F. Probabilistic surrogate networks for simulators with unbounded randomness. In *Uncertainty in Artificial Intelligence*, 2022.

Nye, M., Andreassen, A. J., Gur-Ari, G., Michalewski, H., Austin, J., Bieber, D., Dohan, D., Lewkowycz, A., Bosma, M., Luan, D., Sutton, C., and Odena, A. Show your work: Scratchpads for intermediate computation with language models. *arXiv preprint 2112.00114*, 2021.

OpenAI, :, Achiam, J., Adler, S., Agarwal, S., Ahmad, L., Akkaya, I., Aleman, F. L., Almeida, D., Altenschmidt, J., Altman, S., Anadkat, S., Avila, R., Babuschkin, I., Balaji, S., Balcom, V., Baltescu, P., Bao, H., Bavarian, M., Belgum, J., Bello, I., Berdine, J., Bernadett-Shapiro, G., Berner, C., Bogdonoff, L., Boiko, O., Boyd, M., Brakman, A.-L., Brockman, G., Brooks, T., Brundage, M., Button, K., Cai, T., Campbell, R., Cann, A., Carey, B., Carlson, C., Carmichael, R., Chan, B., Chang, C., Chantzis, F., Chen, D., Chen, S., Chen, R., Chen, J., Chen, M., Chess, B., Cho, C., Chu, C., Chung, H. W., Cummings, D., Currier, J., Dai, Y., Decareaux, C., Degry, T., Deutsch, N., Deville, D., Dhar, A., Dohan, D., Dowling, S., Dunning, S., Ecoffet, A., Eleti, A., Eloundou, T., Farhi, D., Fedus, L., Felix, N., Fishman, S. P., Forte, J., Fulford, I., Gao, L., Georges, E., Gibson, C., Goel, V., Gogineni, T., Goh, G., Gontijo-Lopes, R., Gordon, J., Grafstein, M., Gray, S., Greene, R., Gross, J., Gu, S. S., Guo, Y., Hallacy, C., Han, J., Harris, J., He, Y., Heaton, M., Heidecke, J., Hesse, C., Hickey, A., Hickey, W., Hoeschele, P., Houghton, B., Hsu, K., Hu, S., Hu, X., Huizinga, J., Jain, S., Jain, S., Jang, J., Jiang, A., Jiang, R., Jin, H., Jin, D., Jomoto, S., Jonn, B., Jun, H., Kaftan, T., Łukasz Kaiser, Kamali, A., Kanitscheider, I., Keskar, N. S., Khan, T., Kilpatrick, L., Kim, J. W., Kim, C., Kim, Y., Kirchner, H., Kiros, J., Knight, M., Kokotajlo, D., Łukasz Kondraciuk, Kondrich, A., Konstantinidis, A., Kosic, K., Krueger, G., Kuo, V., Lampe, M., Lan, I., Lee, T., Leike, J., Leung, J., Levy, D., Li, C. M., Lim, R., Lin, M., Lin, S., Litwin, M., Lopez, T., Lowe, R., Lue, P., Makanju, A., Malfacini, K., Manning, S., Markov, T., Markovski, Y., Martin, B., Mayer, K., Mayne, A., McGrew, B., McKinney, S. M., McLeavey, C., McMillan, P., McNeil, J., Medina, D., Mehta, A., Menick, J., Metz, L., Mishchenko, A., Mishkin, P., Monaco, V., Morikawa, E., Mossing, D., Mu, T., Murati, M., Murk, O., Mély, D., Nair, A., Nakano, R., Nayak, R., Neelakantan, A., Ngo, R., Noh, H., Ouyang, L., O'Keefe, C., Pachocki, J., Paino, A., Palermo, J., Pantuliano, A., Parascandolo, G., Parish, J., Parparita, E., Passos, A., Pavlov, M., Peng, A., Perelman, A., de Avila Belbute Peres, F., Petrov, M., de Oliveira Pinto, H. P., Michael, Pokorny, Pokrass, M., Pong, V., Powell, T., Power, A., Power, B., Proehl, E., Puri, R., Radford, A., Rae, J., Ramesh, A., Raymond, C., Real, F., Rimbach, K., Ross, C., Rotsted, B., Roussez, H., Ryder, N., Saltarelli, M., Sanders, T., Santurkar, S., Sastry, G., Schmidt, H., Schnurr, D., Schulman, J., Selsam, D., Sheppard, K., Sherbakov, T., Shieh, J., Shoker, S., Shyam, P., Sidor, S., Sigler, E., Simens, M., Sitkin, J., Slama, K., Sohl, I., Sokolowsky, B., Song, Y., Staudacher, N., Such, F. P., Summers, N., Sutskever, I., Tang, J., Tezak, N., Thompson, M., Tillet, P., Tootoonchian, A., Tseng, E., Tuggle, P., Turley, N., Tworek, J., Uribe, J. F. C., Vallone, A., Vijayvergiya, A., Voss, C., Wainwright, C., Wang, J. J., Wang, A., Wang, B., Ward, J., Wei, J., Weinmann, C., Welihinda, A., Welinder, P., Weng, J., Weng, L., Wiethoff, M., Willner, D., Winter, C., Wolrich, S., Wong, H., Workman, L., Wu, S., Wu, J., Wu, M., Xiao, K., Xu, T., Yoo, S., Yu, K., Yuan, Q., Zaremba, W., Zellers, R., Zhang, C., Zhang, M., Zhao, S., Zheng, T., Zhuang, J., Zhuk, W., and Zoph, B. Gpt-4 technical report. 2023.

Park, J., Amaro, E., Mahajan, D., Thwaites, B., and Esmaeilzadeh, H. Axgames: Towards crowdsourcing quality target determination in approximate computing. 2016.

Pestourie, R., Mroueh, Y., Nguyen, T. V., Das, P., and Johnson, S. G. Active learning of deep surrogates for pdes: application to metasurface design. *npj Computational Materials*, 2020.

Renda, A., Chen, Y., Mendis, C., and Carbin, M. Difftune: Optimizing cpu simulator parameters with learned differentiable surrogates. In *International Symposium on Microarchitecture*, 2020.

Renda, A., Ding, Y., and Carbin, M. Programming with neural surrogates of programs. In *Symposium on New Ideas, New Paradigms, and Reflections on Programming and Software*, 2021.

Sampson, A., Dietl, W., Fortuna, E., Gnanapragasam, D., Ceze, L., and Grossman, D. Enerj: approximate data types for safe and general low-power computation. In *Programming Language Design and Implementation*, 2011.

Shirobokov, S., Belavin, V., Kagan, M., Ustyuzhanin, A., and Baydin, A. G. Black-box optimization with local generative surrogates. In *Advances in Neural Information Processing Systems*, 2020.

Tercan, H., Guajardo, A., Heinisch, J., Thiele, T., Hopmann, C., and Meisen, T. Transfer-learning: Bridging the gap between real and simulation data for machine learning in injection molding. *Procedia CIRP*, 2018.

Tseng, E., Yu, F., Yang, Y., Mannan, F., Arnaud, K. S., Nowrouzezahrai, D., Lalonde, J.-F., and Heide, F. Hyperparameter optimization in black-box image processing using differentiable proxies. *Transactions on Graphics*, 2019.

Turc, I., Chang, M., Lee, K., and Toutanova, K. Well-read students learn better: The impact of student initialization on knowledge distillation. *arXiv preprint 1908.08962*, 2019.

Wang, Z., Bovik, A., Sheikh, H., and Simoncelli, E. Image quality assessment: from error visibility to structural similarity. *IEEE Transactions on Image Processing*, 2004.

Wei, J., Wang, X., Schuurmans, D., Bosma, M., brian ichter, Xia, F., Chi, E. H., Le, Q. V., and Zhou, D. Chain of thought prompting elicits reasoning in large language models. In *Advances in Neural Information Processing Systems*, 2022.

Zaremba, W. and Sutskever, I. Learning to execute. *arXiv preprint 1410.4615*, 2015.

Zhmoginov, A., Sandler, M., and Vladymyrov, M. Hypertransformer: Model generation for supervised and semi-supervised few-shot learning. In *International Conference on Machine Learning*, 2022.

A. Related Work

Our design of neural surrogate compilers for numerical programs draws from the literature on neural surrogates of programs and meta-learning.

A.1. Neural Surrogates of Programs

A common approach to developing neural surrogates of programs is to train a program-specific neural surrogate[3] on a dataset of input-output examples (Renda et al., 2021), or more recently, to train a universal neural surrogate on a dataset that includes many programs (Zaremba & Sutskever, 2015; Nye et al., 2021). Our work presents an alternative method for training neural surrogates of numerical programs that maintains the speed of program-specific neural surrogates but incorporates the data efficiency benefits of universal neural surrogates. Our technique does not provide any guarantees on the suitability of the neural surrogates it produces for downstream tasks; we discuss this issue at the end of this section.

Program-Specific Neural Surrogates. Researchers across scientific disciplines have used neural surrogates of numerical programs to accelerate computations, adapt to new settings, and enable gradient-based optimization. Esmaeilzadeh et al. (2012a) demonstrate that neural surrogates of numerical programs can improve performance for computations in signal processing, robotics, 3D games, compression, machine learning, and image processing. To accelerate optical metasurface design, An et al. (2019) use neural surrogates of numerical simulators and Pestourie et al. (2020) use neural surrogates of partial differential equations. Tercan et al. (2018) and Kustowski et al. (2020) use neural surrogates of numerical simulators for plastic injection molding and inertial confinement fusion, respectively, to facilitate data-efficient finetuning on real physical data. Kaya & Hajimirza (2019) accelerate numerical simulations for solar cells using neural surrogates, and they use transfer learning to quickly adapt neural surrogates when simulator configurations change. Shirobokov et al. (2020) use neural surrogates of non-differentiable, numerical physical simulators, to enable gradient-based optimization of simulator parameters.

Researchers have used nonnumerical surrogates to optimize and explore discrete configuration spaces. Tseng et al. (2019) and Renda et al. (2020) develop neural surrogates of a black-box image signal processing unit and a cycle-accurate CPU simulator, respectively; both techniques enable gradient-based optimization of program inputs, to match some desired input-output behavior. Kwon & Carloni (2020) develop a neural surrogate of a high-level synthesis pipeline for hardware. Using this surrogate, they lower the cost of predicting the performance and cost of hardware configurations, and they use transfer learning to lower the cost of developing neural surrogates for new configuration spaces.

[3] In this section, we emphasize when neural surrogates are program-specific, to contrast with universal neural surrogates.

Universal Neural Surrogates. Researchers have developed universal neural surrogates using a variety of architectures. Early work in this area uses long short-term memory networks to predict the results of executing simple, synthetic Python programs (Zaremba & Sutskever, 2015). Later work uses graph neural networks that model program structure in a similar evaluation setup (Bieber et al., 2020). More recently, researchers have trained Transformer-based models on synthetic datasets of programs or large datasets that include programs (Austin et al., 2021; Nye et al., 2021; OpenAI et al., 2023; Bubeck et al., 2023; Gu et al., 2024).

Assessing Quality. To be useful for a given task, a neural surrogate must achieve a sufficiently low approximation error, and the threshold for this approximation error depends on the task. Our work uses the methodology from Esmaeilzadeh et al. (2012a) to determine what is an acceptable approximation error for PARROTBENCHSHORT programs. AXGAMES is a framework for grounding approximation error in terms of user satisfaction that is agnostic to the choice of approximation technique (Park et al., 2016). Thus, in more general spaces of programs, one could use AXGAMES to determine what is an acceptable approximation error.

A.2. Meta-Learning

Meta-learning can improve data efficiency and transfer learning when there is task-agnostic knowledge that can be extracted from a family of tasks (Hospedales et al., 2022). For example, in the setting we consider, the knowledge of how to execute programs is not specific to any one program but is useful for compiling each program. We describe the technique we employ, hypernetworks (Ha et al., 2017), as well as another meta-learning technique, MAML (model-agnostic meta-learning) (Finn et al., 2017). The most noteworthy difference between the two is that, in the former, the parameter space of the meta-learner and the learners differ, whereas, in the latter, these spaces are the same.

Hypernetworks. Hypernetworks were first proposed by Ha et al. and achieve state-of-the-art results on sequence modeling tasks (Ha et al., 2017). More recent work by Jin et al. proposes a system, N^3, that adapts Transformers to function as hypernetworks that condition on text for few-shot learning on image classification tasks (2020).

Model-Agnostic Meta-Learning. MAML is a framework for developing neural network initializations that can be finetuned to new tasks with a small amount of data and a few iterations of SGD (Finn et al., 2017). Some authors have noted, however, that MAML couples the task space complexity to the complexity of the individual tasks (Zhmoginov et al., 2022), making the parameter space a bottleneck as the task space grows. Our technique does not suffer from this issue because the hypernetwork can be larger than the generated neural surrogate.

B. EXESTACK Data Curation and Filtering

① **Preprocessing.** We pull the functions in EXESTACK from files that may contain preprocessor directives, which may affect the ability for these functions to be executed in isolation, if left unexpanded. We run the C preprocessor on source files until no more lines begin with "#", or we have run it twice, or an invocation fails.

② **Extracting Functions.** Extract any functions from each source file.

③ **Filtering for Pointer-Free Numeric Functions.** To filter for numeric functions in C programs, we only include C functions that use exclusively `float` and `double` data types in the function signature. Due to the possibility of dynamically sized inputs in the presence of pointers and the ambiguity of whether a pointer represents an input or output, we do not allow pointer types. Consequently, we also do not allow `void` as an output type. If checking a file for the above conditions takes longer than 8 seconds, we discard it. Note that these filters still allow integral and pointer data types to be used within the function.

④ **Filtering for Executable Functions and Collecting Outputs.** To simultaneously check for executability and collect outputs from a function, we first generate 2048 sets of inputs by sampling from the uniform distribution $\mathcal{U}(-1, 1)$ and use the same sets of inputs for all programs. We embed these inputs in a C program that includes the function source, as well as an execution harness for collecting outputs. The harness is compiled with the C standard math library included, since many numerical functions in C make use of this library. If there are any errors during compilation or execution of a function, we discard the function. We provide an example of the execution harness instantiated for a function in Appendix C.

To target a fixed neural surrogate architecture, a methodology is required for interpreting functions of varying type signatures as a single, fixed type signature. For a neural surrogate architecture with m inputs and n outputs, we distinguish the first m arguments of a function as the input for the neural surrogate, and we initialize all other arguments to the constant 1.0. When a function has more than n outputs, we only collect the first n outputs. When a function has fewer than n outputs, we pad the function outputs with the constant 0.0.

```c
#include <stdlib.h>
#include <stdio.h>
#include <math.h>

float inputs[1024][1] = {
  {0.10740153873327762},
  ...
};

float fftSin(float x) {
    return sin(-2 * 3.1415 * x);
}

int main() {
    for (int i = 0; i < 1024; i++) {
        float arg0 = inputs[i][0];
        float out = fftSin(arg0);
        printf("%f,", out);
        printf("\n");
    }
    return 0;
}
```

Figure 8: Source code template used for checking executability and collecting outputs, instantiated with the source of `fftSin`.

⑤ **Filtering for Deterministic Functions.** Since a neural surrogate is often a deterministic function of its inputs and weights, we filter nondeterministic functions from our dataset. We check for determinism by running a function 5 times on the same inputs, all sampled from $\mathcal{U}(-1, 1)$, and observing whether the output differs on any execution.

⑥ **Deduplication.** We use a whitespace-invariant tokenizer to remove duplicate tokenized programs.

C. EXESTACK Execution Harness

Figure 8 shows an example of the execution harness we use to collect outputs from functions for EXESTACK.

D. EXESTACKCPN Generation

To produce EXESTACKCPN, we apply the following additional filters to EXESTACK:

- **Filtering Long Programs.** Since BERT-Tiny has a maximum context length of 512 tokens, we remove functions with more than 512 tokens. We first strip comments from all programs to allow more programs to fit within the context.
- **Filtering Large Outputs.** Large or NaN outputs can lead to training instability for neural networks, so we

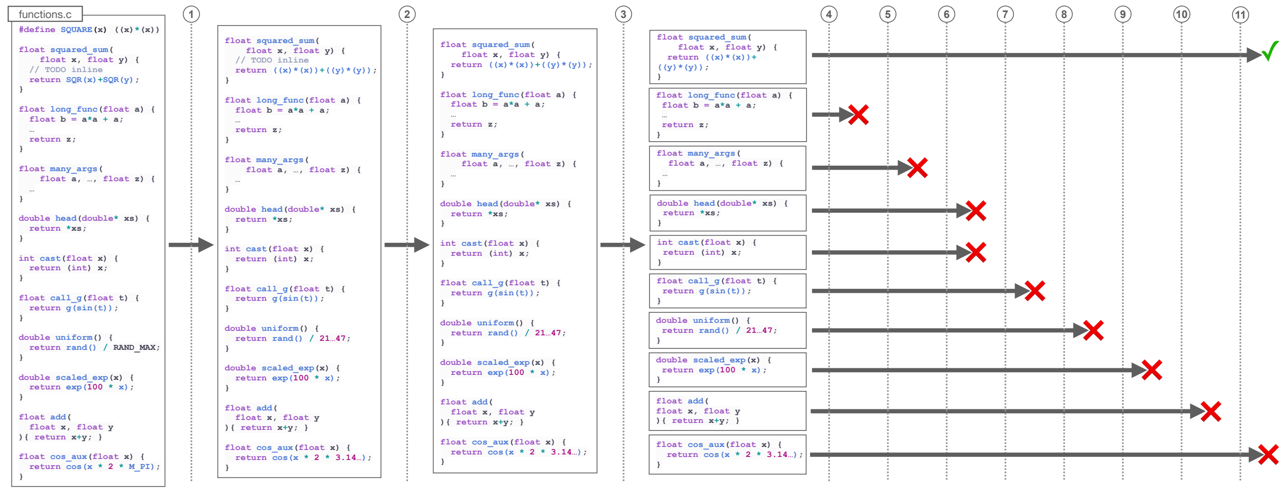

```
#define SQUARE(x) ((x)*(x))

float squared_sum(
    float x, float y) {
  // TODO inline
  return SQR(x)+SQR(y);
}

float long_func(float a) {
  float b = a*a + a;
  …
  return z;
}

float many_args(
    float a, …, float z) {
  …
}

double head(double* xs) {
  return *xs;
}

int cast(float x) {
  return (int) x;
}

float call_g(float t) {
  return g(sin(t));
}

double uniform() {
  return rand() / RAND_MAX;
}

double scaled_exp(x) {
  return exp(100 * x);
}

float add(
  float x, float y
){ return x+y; }

float cos_aux(float x) {
  return cos(x * 2 * M_PI);
}
```

```
float squared_sum(
    float x, float y) {
  // TODO inline
  return ((x)*(x))+((y)*(y));
}

float long_func(float a) {
  float b = a*a + a;
  …
  return z;
}

float many_args(
    float a, …, float z) {
  …
}

double head(double* xs) {
  return *xs;
}

int cast(float x) {
  return (int) x;
}

float call_g(float t) {
  return g(sin(t));
}

double uniform() {
  return rand() / 21…47;
}

double scaled_exp(x) {
  return exp(100 * x);
}

float add(
  float x, float y
){ return x+y; }

float cos_aux(float x) {
  return cos(x * 2 * 3.14…);
}
```

```
float squared_sum(
    float x, float y) {
  return ((x)*(x))+((y)*(y));
}

float long_func(float a) {
  float b = a*a + a;
  …
  return z;
}

float many_args(
    float a, …, float z) {
  …
}

double head(double* xs) {
  return *xs;
}

int cast(float x) {
  return (int) x;
}

float call_g(float t) {
  return g(sin(t));
}

double uniform() {
  return rand() / 21…47;
}

double scaled_exp(x) {
  return exp(100 * x);
}

float add(
  float x, float y
){ return x+y; }

float cos_aux(float x) {
  return cos(x * 2 * 3.14…);
}
```

```
float squared_sum(
    float x, float y) {
  return ((x)*(x))+
((y)*(y));
}
```

```
float long_func(float a) {
 float b = a*a + a;
 …
 return z;
}
```

```
float many_args(
  float a, …, float z) {
 …
}
```

```
double head(double* xs) {
 return *xs;
}
```

```
int cast(float x) {
 return (int) x;
}
```

```
float call_g(float t) {
 return g(sin(t));
}
```

```
double uniform() {
 return rand() / 21…47;
}
```

```
double scaled_exp(x) {
 return exp(100 * x);
}
```

```
float add(
float x, float y
){ return x+y; }
```

```
float cos_aux(float x) {
  return cos(x * 2 * 3.14…);
}
```

Figure 9: The EXESTACKCPN generation pipeline (i.e., EXESTACK tailored to COMPNETS). Starting with C source files from The Stack, we apply a sequence of maps followed by a sequence of filters. The steps are (1) run the C preprocessor, (2) remove comments, (3) extract functions from the source file, (4) remove functions with more tokens than a user-specified threshold (e.g., the maximum context length), (5) remove functions with more inputs than the target topology, (6) remove functions with pointers in their type signature and nonnumeric functions, (7) remove nonexecutable functions and collect input-output pairs, (8) remove nondeterministic functions, (9) remove functions with any outputs larger than a user-specified threshold, when run on the set of input-output pairs, (10) remove any duplicate programs, and (11) remove any programs syntactically similar to programs in PARROTBENCHSHORT. Red "X"s denote that a function does not pass a filter and green checkmarks denote that a function passes all filters.

additionally remove functions with any outputs with an absolute magnitude of 10 or larger or a NaN value.

- **Decontaminating Against PARROTBENCHSHORT.** It is possible that EXESTACK contains similar programs to those in PARROTBENCHSHORT. If we trained a COMPNET on these programs, improvements over random initialization could be due to memorization. To address this problem, we remove any programs from EXESTACK that are syntactically similar to programs in PARROTBENCHSHORT.

Characteristic	Value
Max Program Length (In Tokens)	512
Tokenizer Vocab Size	30,522
# Programs in Dataset	37,772
# Tokens in Dataset	1,728,304
# I/O Pairs Per Program	2,048

Figure 10: Summary of EXESTACKCPN characteristics.

E. EXESTACKCPN Generation (Extended)

In this appendix, we present an example showing the entire pipeline for generating EXESTACKCPN (Figure 9), a summary of EXESTACKCPN characteristics (Figure 10), a histogram showing the distribution of arity among `ExeStackCPN` programs (Figure 11), and we detail the decontamination step (Section E.1).

E.1. EXESTACKCPN Decontamination

To ensure the improvements observed in Section 5 are not due to memorization, the final step of EXESTACKCPN generation is decontamination against PARROTBENCHSHORT programs. A prevailing decontamination methodology in the literature is to remove any syntactic matches up to whitespace (Li et al., 2022; Lozhkov et al., 2024). Though EXESTACK is not contaminated with PARROTBENCHSHORT programs according to this methodology, we strengthen our methodology to additionally remove syntactically similar programs. This decontamination consists of bespoke syntactic analyses—one for each PARROTBENCHSHORT program. For the remainder of this section, we present each of these syntactic analyses and a sample of the programs they mark for removal. In total, decontamination removes 375 functions.

E.1.1. FFT (OUTPUT 0)

Recall, the source for the `fft (0)` kernel in PARROTBENCHSHORT is

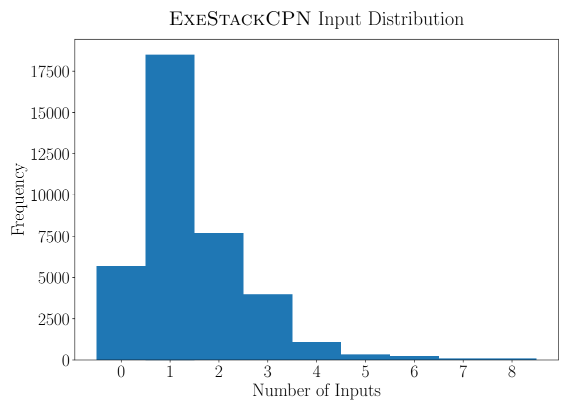

Figure 11: Distribution of the number of program inputs for programs in ExeStackCPN.

```
float fftSin_Output0(float x) {
    return sin(-2 * 3.1415 * x);
}
```

To decontaminate ExeStackCPN against this program, we search for programs satisfying all conditions below:

- Contains “sin”
- Contains either “3.14” or “M_PI”
- Is at most 5 (non-empty) lines long
- Has one input

This methodology surfaces 29 matches. Below, we include a sample of 5 of these matches:

```
float seno(float x) {
  return sin(x * M_PI / 180);
}

float exponential(float value) {
  return sin(value * 3.14f / 2);
}

float easeOutSine(float time) {
  return sin(time * M_PI / 2);
}

double sine(double t) {
  return sin(2 * M_PI * t);
}

double cosine(double t) {
  return cos(2 * M_PI * t);
}
```

E.1.2. FFT (Output 1)

Recall, the source for the `fft (1)` kernel in ParrotBenchShort is

```
float fftSin_Output1(float x) {
    return cos(-2 * 3.1415 * x);
}
```

To decontaminate ExeStackCPN against this program, we search for programs satisfying all conditions below:

- Contains “cos”
- Contains either “3.14” or “M_PI”
- Is at most 5 (non-empty) lines long
- Has one input

This methodology surfaces 20 matches. Below, we include a sample of 5 of these matches:

```
float coss(float x) {
  return cos(x * M_PI / 180);
}

double cosine(double t) {
  return cos(2 * M_PI * t);
}

float hamming(float x) {
  return 0.54-0.46*cos(2*M_PI*x);
}

float easeInSine(float time) {
  return 1 - cos(time * M_PI / 2);
}

float easeInOutSine(float time) {
  return 0.5 * (1 - cos(M_PI * time));
}
```

E.2. InverseK2J (Output 0)

Recall, the source for the `invk2j (0)` kernel in ParrotBenchShort is

```
float inversek2j_Output0(
    float x, float y) {
  float l1 = 0.5 ;
  float l2 = 0.5 ;
  float theta2 = (float) acos(
    ((x * x) + (y * y) -
      (l1 * l1) -
      (l2 * l2)) /
    (2 * l1 * l2)
  );
  return (float) asin(
    (y * (l1 + l2 * cos(theta2)) -
      x * l2 * sin(theta2)) /
    (x * x + y * y)
  );
}
```

To decontaminate EXESTACKCPN against this program, we search for programs satisfying all conditions below:

- Contains “asin”, “acos”, “sin”, and “cos”
- Contains either “.5” or (“/” and “2”)
- Is at most 7 (non-empty) lines long
- Has two inputs

This methodology surfaces 0 matches.

E.3. InvK2J (Output 1)

Recall, the source for the `invk2j (1)` kernel in PARROTBENCHSHORT is

```
float inversek2j_Output1(
    float x, float y) {
  float l1 = 0.5 ;
  float l2 = 0.5 ;
  return (float) acos(
    ((x * x) + (y * y) -
      (l1 * l1) - (l2 * l2)) /
    (2 * l1 * l2)
  );
}
```

To decontaminate EXESTACKCPN against this program, we search for programs satisfying all conditions below:

- Contains “acos”
- Contains either “.5” or (“/” and “2”)
- Is at most 6 (non-empty) lines long
- Has two inputs

This methodology surfaces 0 matches.

E.3.1. KMEANS

Recall, the source for the `kmeans` kernel in PARROTBENCHSHORT is

```
float euclideanDistance(
    float p_0, float p_1, float p_2,
    float c1_0, float c1_1, float c1_2) {
  float r;

  r = 0;
  r += (p_0 - c1_0) * (p_0 - c1_0);
  r += (p_1 - c1_1) * (p_1 - c1_1);
  r += (p_2 - c1_2) * (p_2 - c1_2);

  return sqrt(r);
}
```

To decontaminate EXESTACKCPN against this program, we search for programs satisfying all conditions below:

- Contains “sqrt”, “*”, “+”, and “-”
- Has 6 inputs

This methodology surfaces 10 matches. Below, we include a sample of 5 of these matches:

```
float len(
  float x0, float y0, float z0,
  float x1, float y1, float z1 ){
    return sqrt(
      (x1-x0)*(x1-x0) +
      (y1-y0)*(y1-y0) +
      (z1-z0)*(z1-z0)
    );
}

float dist(
    float x1, float y1,float z1,
    float x2,float y2,float z2) {
  return sqrt(
    (x1-x2)*(x1-x2) +
    (y1-y2)*(y1-y2) +
    (z1-z2)*(z1-z2)
  );
}

float calc_dist(
    float x0, float y0, float z0,
    float x1, float y1, float z1) {
  float dx   = (x1 - x0);
  float dy   = (y1 - y0);
  float dz   = (z1 - z0);
  float dist = sqrtf(
    (dx * dx) +
    (dy * dy) +
    (dz * dz)
  );
  return dist;
}

double dist(
    double x0, double y0, double z0,
    double x1, double y1, double z1) {
  return sqrt(
    (x1 - x0) * (x1 - x0) +
    (y1 - y0) * (y1 - y0) +
    (z1 - z0) * (z1 - z0)
  );
}

double dist(
    double ax, double ay, double az,
    double bx, double by, double bz) {
  return sqrt(
    (ax - bx)*(ax - bx) +
    (ay - by)*(ay - by) +
    (az - bz)*(az - bz)
  );
}
```

E.3.2. SOBEL

Recall, the source for the `sobel` kernel in PARROTBENCHSHORT is

```
float sobel(
    float w00, float w01, float w02,
    float w10, float w11, float w12,
    float w20, float w21, float w22) {
  float sx = 0.0;
  sx += w00 * -1;
  sx += w10 * 0;
  sx += w20 * 1;
  sx += w01 * -2;
  sx += w11 * 0;
  sx += w21 * 2;
  sx += w02 * -1;
  sx += w12 * 0;
  sx += w22 * 1;

  float sy = 0.0;
  sy += w00 * -1;
  sy += w10 * -2;
  sy += w20 * -1;
  sy += w01 * 0;
  sy += w11 * 0;
  sy += w21 * 0;
  sy += w02 * 1;
  sy += w12 * 2;
  sy += w22 * 1;

  float s = sqrt(
    sx * sx + sy * sy);
  if (s >= (256 / sqrt(
      256 * 256 + 256 * 256)))
    s = 255 / sqrt(
      256 * 256 + 256 * 256);
  return s;
}
```

To decontaminate EXESTACKCPN against this program, we search for programs satisfying all conditions below:

- Contains “sqrt”, “+”, “*”, and “/”
- Has 9 inputs

This methodology surfaces 0 matches.

F. Parrot Dataset Details

Due to methodological choices in EXESTACK and architectural choices for COMPNETS, we omit some PARROTBENCH benchmarks from PARROTBENCHSHORT and modify others. We omit the `jmeint` and `jpeg` benchmarks in PARROTBENCH because they are significantly longer than the 512-token context length of a BERT-Tiny (1,192 and 1,250 tokens, respectively). We modify the `fft` and `invk2j` benchmarks because they both use pointer arguments to store outputs, and our COMPNETS were not trained to support pointer arguments. To make each function pointer-free, we split it into two functions, each function computing one of the outputs[4]. Additionally, the `sobel` benchmark uses pointer inputs, so we rewrite it to only use scalar inputs. Finally, the `kmeans` benchmark uses custom structs to pass arguments, so we rewrite the benchmark to desugar these structs into their scalar components.

We list the modified code for each benchmark in Appendix F.1, and we describe how we generate inputs for these programs in Appendix F.2.

F.1. PARROTBENCHSHORT Code

We present the code used for PARROTBENCHSHORT in our evaluation (Section 5), which we adapted from PARROTBENCH to be pointer-free. The code for the benchmarks is shown in Figures 12, 13, 14, and 15.

F.2. ParrotBenchShort Input Generation

Here, we detail how we generated inputs for PARROTBENCHSHORT programs. We attempt to exactly replicate the dataset used by Esmaeilzadeh et al. (2012a) for the subset of benchmarks we consider from PARROTBENCH.

[4] As described in Section 3, we use the first output of each function to produce an initialization for the original function.

```
float fftSin_Output0(float x) {
    return sin(-2 * 3.1415 * x);
}

float fftSin_Output1(float x) {
    return cos(-2 * 3.1415 * x);
}
```

Figure 12: Code for the `fft` benchmark in PARROTBENCHSHORT.

```
float invk2j_Output0(float x, float y) {
  float l1 = 0.5 ;
  float l2 = 0.5 ;
  float theta2 = (float)acos(
    ((x * x) + (y * y) - (l1 * l1) - (l2 * l2)) /
    (2 * l1 * l2)) ;
  return (float)asin(
    (y * (l1 + l2 * cos(theta2)) - x * l2 * sin(theta2)) /
    (x * x + y * y)) ;
}

float invk2j_Output1(float x, float y) {
  float l1 = 0.5 ;
  float l2 = 0.5 ;
  return (float)acos(
    ((x * x) + (y * y) - (l1 * l1) - (l2 * l2)) /
    (2 * l1 * l2)) ;
}
```

Figure 13: Code for the `invk2j` benchmark in PARROTBENCHSHORT.

```
float euclideanDistance(
  float p_0, float p_1, float p_2,
  float c1_0, float c1_1, float c1_2) {
  float r;

  r = 0;
  r += (p_0 - c1_0) * (p_0 - c1_0);
  r += (p_1 - c1_1) * (p_1 - c1_1);
  r += (p_2 - c1_2) * (p_2 - c1_2);

  return sqrt(r);
}
```

Figure 14: Code for the `kmeans` benchmark in PARROTBENCHSHORT.

```
float sobel(
  float w00, float w01, float w02,
  float w10, float w11, float w12,
  float w20, float w21, float w22)
{
  float sx = 0.0;
  sx += w00 * -1;
  sx += w10 * 0;
  sx += w20 * 1;
  sx += w01 * -2;
  sx += w11 * 0;
  sx += w21 * 2;
  sx += w02 * -1;
  sx += w12 * 0;
  sx += w22 * 1;

  float sy = 0.0;
  sy += w00 * -1;
  sy += w10 * -2;
  sy += w20 * -1;
  sy += w01 * 0;
  sy += w11 * 0;
  sy += w21 * 0;
  sy += w02 * 1;
  sy += w12 * 2;
  sy += w22 * 1;

  float s = sqrt(sx * sx + sy * sy) ;
  if (s >= (256 / sqrt(256 * 256 + 256 * 256)))
    s = 255 / sqrt(256 * 256 + 256 * 256);
  return s ;
}
```

Figure 15: Code for the `sobel` benchmark in PARROTBENCHSHORT.

Figure 16: Image used to generate testing data for `kmeans`.

F.2.1. FFT

To generate train inputs for `fft`, we generate 32,768 inputs uniformly at random from $[0, 1/2]$. To generate test inputs for `fft`, we generate 2,048 inputs uniformly at random from $[0, 1/2]$, resampling as necessary whenever an input is generated that exists in the train set.

F.2.2. INVERSEK2J

To generate train inputs for `invk2j`, we generate 10,000 inputs uniformly at random from $[-1/2, 1] \times [0, 1]$. To generate test inputs for `invk2j`, we generate 10,000 inputs uniformly at random from $[-1/2, 1] \times [0, 1]$, resampling as necessary whenever an input is generated that exists in the train set.

F.2.3. KMEANS

To generate train inputs for `kmeans`, we generate 50,000 inputs uniformly at random from $[0, 1]^6$.

To generate test inputs for `kmeans`, we use an image of peppers for RGB inputs (see Figure 16) and we generate 6 centroids with uniformly random coordinates in $[0, 1]$, the number of centroids used by Esmaeilzadeh et al. (source). For each RGB input, we then choose a random centroid to compute the `kmeans` kernel on, and we add the resulting I/O sample to the test set. This procedure results in 48,400 inputs.

F.2.4. SOBEL

To generate train and test inputs for `sobel`, we read from files on the official repo of Esmaeilzadeh et al. (2012a) (here and here, respectively). These files contain 18,725 and 17,976 input-output pairs, respectively.

G. COMPNET Training Details

COMPNETS are controlled by the following hyperparameters: program batch size, input batch size, learning rate, number of training epochs, dataset program split, dataset input split, and the surrogate topology. We swept over learning rates and chose fixed values for all other hyperparameters. We selected the learning rate that achieved the best final loss on test programs, and we used all 3 trials of the winning configuration as initialization methods. We summarize the training configuration for pretrained surrogates in Figure 17.

H. MAML Training Details

MAML is controlled by the following hyperparameters: the meta batch size (number of tasks per batch), the input batch size (number of inputs per task), the number of epochs, the inner gradient update step size (α), the outer gradient update step size (β), and the number of inner gradient update steps.

We chose the meta batch size and the input batch size to align with how we trained COMPNETS (Appendix G). We decided to use the maximum number of epochs Finn et al. (2017) use in their applications ($70,000$), and we observed that in all applications, β is fixed at 0.001. For the remaining parameters, α and the number of inner update steps, we performed a hyperparameter sweep, backing each configuration with 3 trials. We chose the extents of each hyperparameter in the sweep as the minimum and maximum of hyperparameter settings observed in applications, and we added some points between these extents. However, we limited the hyperparameter settings for α to a maximum of 0.2, as previous experiments (not reported in this paper) showed training instability at higher values.

After each configuration finished training, we finetuned it for 20 epochs for each of a sample of 5 programs from the EXESTACKCPN validation set. We chose the hyperparameters with the lowest loss on the validation inputs at the end of finetuning, averaged over the sample of programs and trials. We used all 3 trials of the winning configuration as initialization methods.

We summarize the training configuration for MAML in Figure 18.

I. Pretrained Neural Surrogate Training Details

Similarly to COMPNETS, pretrained surrogates are controlled by the following hyperparameters: program batch size, input batch size, learning rate, number of training epochs, dataset program split, dataset input split, and the surrogate topology. We swept over the same set of learning rates as we did for COMPNETS, and we use the same values for other hyperparameters that we did for COMPNETS. We selected the learning rate that achieved the best final loss on test programs, and we used all 3 trials of the winning configuration as initialization methods. We summarize the training configuration for pretrained surrogates in Figure 19.

Setting	Value
Architecture	BERT-Tiny
Program Batch Size	32
Input Batch Size	1024
Learning Rate	$\in \{\mathbf{1 \cdot 10^{-5}}, 2 \cdot 10^{-5}, 5 \cdot 10^{-5}, 5 \cdot 10^{-4}, 8 \cdot 10^{-4}\}$
# Epochs	$1,500$
Dataset Program Split	$80/0/20$
Dataset Input Split	$50/0/50$
Surrogate Topology	$9 \to 4 \to 4 \to 1$
GPU	NVIDIA Tesla T4 16GB
# Trials	3

Figure 17: Training configuration for COMPNETS. We represent any values we sweep over as a set, and we bold the values that obtain the best final loss on test programs.

Setting	Value
Meta Batch Size	32
Input Batch Size	1024
# Epochs	$70,000$
α	$\in \{0.01, 0.05, 0.1, \mathbf{0.2}\}$
β	0.001
# Inner Update Steps	$\in \{1, 2, \mathbf{3}, 4, 5\}$
# Finetuning Epochs	20
# Trials	3
Dataset Program Split	80/10/10
Dataset Input Split	50/20/30
Surrogate Topology	$9 \to 4 \to 4 \to 1$
GPU	NVIDIA Tesla T4 16GB

Figure 18: Training configuration for MAML. We represent any values we sweep over as a set, and we bold the values that obtain the best finetuning loss on validation programs.

J. Data Efficiency Improvements (Extended)

The improvements in the data efficiency evaluation are computed as a ratio of the test loss achieved by random initialization over the test loss achieved by an initialization method. Here, we present the test losses used to compute these ratios.

Figure 20 contains histograms showing, for a sample of 1,000 EXESTACKCPN test programs, the test loss each initialization method achieves at the epoch with the lowest validation loss. Figure 21 contains similar plots for PARROTBENCHSHORT programs.

K. Neural Surrogates for Color Quantization (Extended)

In this section, we present quantitative results for a 10- and 15-color palette (Figures 22 and 23).

L. Training Time Improvements

To assess whether COMPNETS improve training time of neural surrogates, we use COMPNETS to initialize neural surrogates, finetune on training data until they reach a target test loss, then compare the results to those of other initialization methods. We first detail the methodology of this experiment, then present results.

L.0.1. METHODOLOGY

We now describe the methodology for setting a target test loss to use as a stopping condition and for selecting configurations to sweep over.

Setting a Target Test Loss. We set a target test loss for each program by training 9 randomly initialized surrogates for 5,000 epochs. The average final test loss is the target test loss for all initialization methods.

Experiment Configurations. In this experiment, we sweep over configurations consisting of a program and an initialization method. Given a program and initialization method, we produce a neural surrogate initialization. We then train the initialized neural surrogate on the training input set until it reaches the target test loss or until it reaches 15,000 epochs. We call whichever epoch comes first the *finish epoch* for the trial.

Quantifying Improvements. We define the improvement for a given configuration (consisting of a program and initialization method) as the ratio of the finish epoch for random initialization and the finish epoch by the configuration's initialization method. All finish epochs are averaged over trials (using arithmetic mean) prior to computing ratios. For each initialization method, we report the geometric mean of the improvements grouped by program, grouped by dataset size, and overall. For some programs and initialization methods, the resulting surrogates achieve losses of 0. We

Setting	Value
Program Batch Size	32
Input Batch Size	1024
Learning Rate	$\in \{\mathbf{1 \cdot 10^{-5}}, 2 \cdot 10^{-5}, 5 \cdot 10^{-5}, 5 \cdot 10^{-4}, 8 \cdot 10^{-4}\}$
# Epochs	$1,500$
Dataset Program Split	$80/0/20$
Dataset Input Split	$50/0/50$
Surrogate Topology	$9 \rightarrow 4 \rightarrow 4 \rightarrow 1$
GPU	NVIDIA Tesla T4 16GB
# Trials	3

Figure 19: Training configuration for pretrained surrogates. We represent any values we sweep over as a set, and we bold the values that obtain the best final loss on test programs.

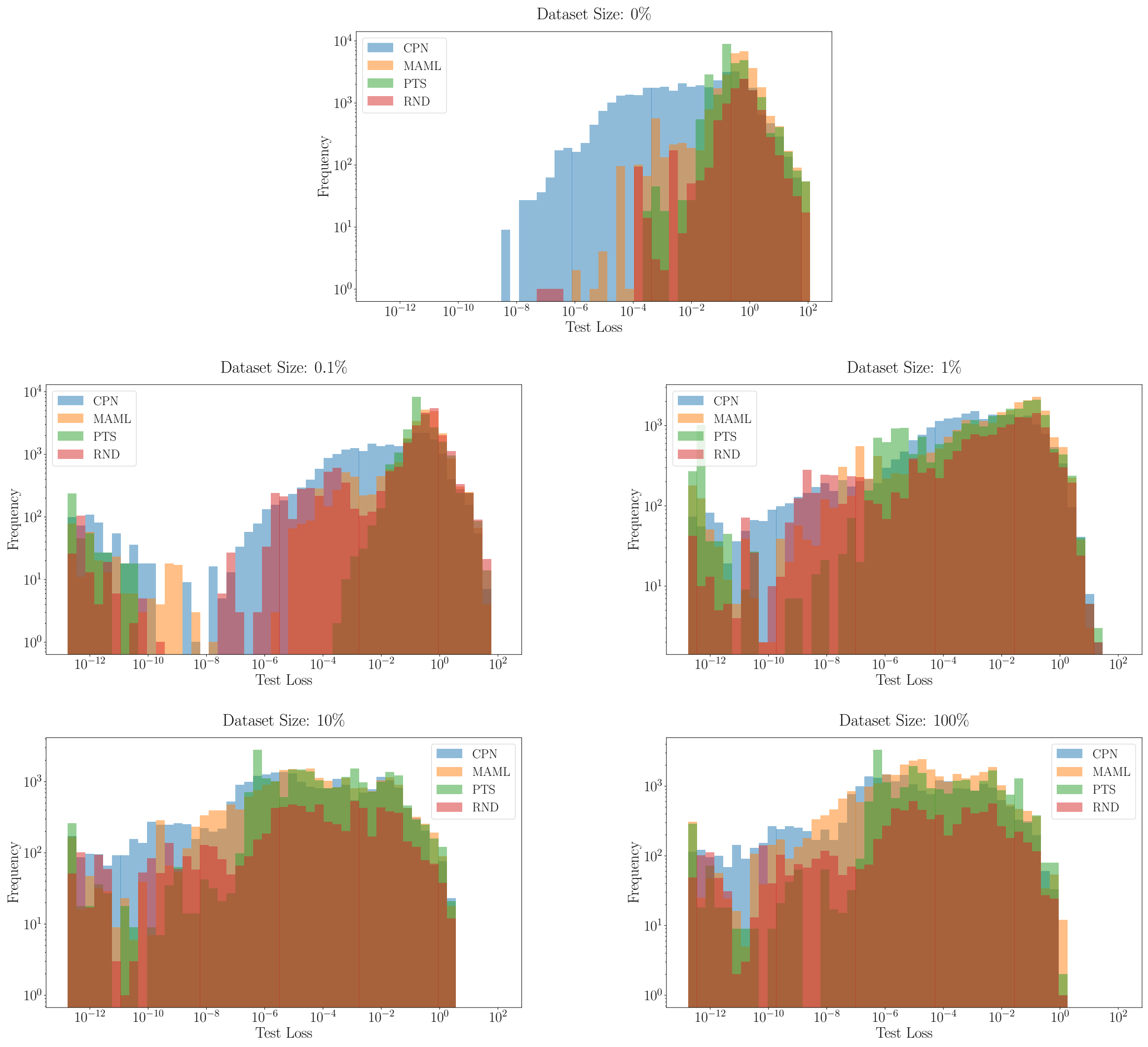

Figure 20: Histograms showing test losses of each initialization method at the epoch with the lowest validation loss for EXESTACKCPN test programs.

Dataset Size 0%				
Program	CPN	MAML	PTS	RND
`fft`	1.3 ± 1.2	0.6 ± 0.2	0.8 ± 0.1	0.6 ± 0.3
`invk2j`	1.8 ± 0.6	2.0 ± 0.6	2.1 ± 0.5	2.4 ± 0.8
`kmeans`	$0.1 \pm 6.7 \cdot 10^{-3}$	0.7 ± 0.4	$0.1 \pm 7.4 \cdot 10^{-4}$	0.2 ± 0.2
`sobel`	$0.1 \pm 3.0 \cdot 10^{-2}$	0.2 ± 0.2	$0.2 \pm 3.5 \cdot 10^{-3}$	0.4 ± 0.3

Dataset Size 0.1%				
Program	CPN	MAML	PTS	RND
`fft`	$7.8 \cdot 10^{-5} \pm 1.1 \cdot 10^{-4}$	$1.9 \cdot 10^{-4} \pm 2.4 \cdot 10^{-4}$	$2.3 \cdot 10^{-4} \pm 4.6 \cdot 10^{-4}$	$1.6 \cdot 10^{-4} \pm 1.1 \cdot 10^{-4}$
`invk2j`	0.2 ± 0.2	0.2 ± 0.2	0.2 ± 0.2	0.3 ± 0.3
`kmeans`	$1.3 \cdot 10^{-2} \pm 1.5 \cdot 10^{-2}$	$0.1 \pm 2.9 \cdot 10^{-2}$	$3.3 \cdot 10^{-2} \pm 1.6 \cdot 10^{-2}$	$3.9 \cdot 10^{-2} \pm 2.1 \cdot 10^{-2}$
`sobel`	$0.1 \pm 2.0 \cdot 10^{-2}$	$4.7 \cdot 10^{-2} \pm 2.1 \cdot 10^{-2}$	$0.1 \pm 2.3 \cdot 10^{-2}$	$0.1 \pm 1.9 \cdot 10^{-2}$

Dataset Size 1%				
Program	CPN	MAML	PTS	RND
`fft`	$3.6 \cdot 10^{-5} \pm 2.7 \cdot 10^{-5}$	$4.6 \cdot 10^{-5} \pm 2.2 \cdot 10^{-5}$	$1.0 \cdot 10^{-4} \pm 1.4 \cdot 10^{-4}$	$4.9 \cdot 10^{-5} \pm 2.8 \cdot 10^{-5}$
`invk2j`	$1.5 \cdot 10^{-2} \pm 4.7 \cdot 10^{-3}$	$1.2 \cdot 10^{-2} \pm 3.7 \cdot 10^{-3}$	$1.3 \cdot 10^{-2} \pm 3.8 \cdot 10^{-3}$	$1.2 \cdot 10^{-2} \pm 3.9 \cdot 10^{-3}$
`kmeans`	$4.7 \cdot 10^{-3} \pm 5.9 \cdot 10^{-3}$	$1.5 \cdot 10^{-2} \pm 1.1 \cdot 10^{-2}$	$1.3 \cdot 10^{-2} \pm 9.3 \cdot 10^{-3}$	$1.3 \cdot 10^{-2} \pm 1.3 \cdot 10^{-2}$
`sobel`	$8.3 \cdot 10^{-3} \pm 4.9 \cdot 10^{-3}$	$8.1 \cdot 10^{-3} \pm 2.8 \cdot 10^{-3}$	$9.1 \cdot 10^{-3} \pm 3.2 \cdot 10^{-3}$	$6.0 \cdot 10^{-3} \pm 3.2 \cdot 10^{-3}$

Dataset Size 10%				
Program	CPN	MAML	PTS	RND
`fft`	$6.4 \cdot 10^{-6} \pm 9.0 \cdot 10^{-6}$	$1.2 \cdot 10^{-5} \pm 1.2 \cdot 10^{-5}$	$1.4 \cdot 10^{-5} \pm 1.5 \cdot 10^{-5}$	$1.3 \cdot 10^{-5} \pm 1.6 \cdot 10^{-5}$
`invk2j`	$8.1 \cdot 10^{-3} \pm 1.4 \cdot 10^{-3}$	$6.5 \cdot 10^{-3} \pm 1.7 \cdot 10^{-3}$	$7.2 \cdot 10^{-3} \pm 1.3 \cdot 10^{-3}$	$7.3 \cdot 10^{-3} \pm 1.4 \cdot 10^{-3}$
`kmeans`	$3.9 \cdot 10^{-3} \pm 5.0 \cdot 10^{-3}$	$1.3 \cdot 10^{-2} \pm 7.9 \cdot 10^{-3}$	$7.8 \cdot 10^{-3} \pm 7.0 \cdot 10^{-3}$	$1.3 \cdot 10^{-2} \pm 1.1 \cdot 10^{-2}$
`sobel`	$1.7 \cdot 10^{-3} \pm 1.7 \cdot 10^{-3}$	$1.6 \cdot 10^{-3} \pm 1.4 \cdot 10^{-3}$	$2.6 \cdot 10^{-3} \pm 1.9 \cdot 10^{-3}$	$1.8 \cdot 10^{-3} \pm 1.6 \cdot 10^{-3}$

Dataset Size 100%				
Program	CPN	MAML	PTS	RND
`fft`	$2.2 \cdot 10^{-6} \pm 5.4 \cdot 10^{-6}$	$1.7 \cdot 10^{-6} \pm 3.1 \cdot 10^{-6}$	$4.2 \cdot 10^{-6} \pm 5.6 \cdot 10^{-6}$	$1.1 \cdot 10^{-6} \pm 1.1 \cdot 10^{-6}$
`invk2j`	$3.3 \cdot 10^{-3} \pm 1.5 \cdot 10^{-4}$	$3.3 \cdot 10^{-3} \pm 6.5 \cdot 10^{-4}$	$3.4 \cdot 10^{-3} \pm 7.2 \cdot 10^{-4}$	$3.0 \cdot 10^{-3} \pm 4.8 \cdot 10^{-4}$
`kmeans`	$3.4 \cdot 10^{-3} \pm 4.7 \cdot 10^{-3}$	$1.4 \cdot 10^{-2} \pm 9.5 \cdot 10^{-3}$	$5.2 \cdot 10^{-3} \pm 4.8 \cdot 10^{-3}$	$8.1 \cdot 10^{-3} \pm 4.3 \cdot 10^{-3}$
`sobel`	$5.3 \cdot 10^{-4} \pm 7.9 \cdot 10^{-5}$	$4.6 \cdot 10^{-4} \pm 1.1 \cdot 10^{-4}$	$6.3 \cdot 10^{-4} \pm 8.5 \cdot 10^{-5}$	$4.1 \cdot 10^{-4} \pm 8.1 \cdot 10^{-5}$

Figure 21: Average test loss achieved by each initialization method on the epoch with the best validation loss for PARROTBENCHSHORT programs. We include a table for each dataset size we evaluated on.

Dataset Size	CPN	MAML	PTS	RND
0%	$2.87e + 03 \pm 615.51$	$3.03e + 03 \pm 394.17$	$3.28e + 03 \pm 129.80$	$3.30e + 03 \pm 0.00e + 00$
0.1%	979.89 ± 853.36	$1.90e + 03 \pm 594.49$	$1.72e + 03 \pm 793.42$	$1.46e + 03 \pm 583.15$
1%	410.61 ± 194.59	677.16 ± 267.41	631.44 ± 226.17	615.89 ± 298.99
10%	401.29 ± 181.23	639.63 ± 169.99	576.00 ± 252.33	631.13 ± 317.59
100%	395.45 ± 184.18	627.57 ± 237.83	498.93 ± 229.30	510.32 ± 154.20

Dataset Size	CPN	MAML	PTS	RND
0%	0.28 ± 0.13	0.20 ± 0.04	0.19 ± 0.03	$0.19 \pm 0.00e + 00$
0.1%	0.60 ± 0.16	0.42 ± 0.12	0.45 ± 0.16	0.49 ± 0.09
1%	0.73 ± 0.10	0.63 ± 0.11	0.64 ± 0.09	0.66 ± 0.12
10%	0.74 ± 0.10	0.62 ± 0.07	0.66 ± 0.12	0.65 ± 0.14
100%	0.74 ± 0.10	0.63 ± 0.11	0.69 ± 0.12	0.68 ± 0.09

Figure 22: Quantitative comparison of end-to-end results produced by various initialization methods on color quantization with a palette size of 10 colors. **(Top)** The average mean squared error (MSE) of the image produced by each initialization method compared to the image produced by a ground-truth implementation of the `kmeans` kernel (lower is better). **(Bottom)** The average structural similarity index measure (SSIM) of the image produced by each initialization method compared to the image produced by a ground-truth implementation of the `kmeans` kernel (higher is better).

Dataset Size	CPN	MAML	PTS	RND
0%	$2.74e + 03 \pm 506.25$	$3.12e + 03 \pm 386.19$	$3.39e + 03 \pm 81.07$	$3.40e + 03 \pm 0.00e + 00$
0.1%	906.06 ± 782.02	$1.84e + 03 \pm 633.11$	$1.74e + 03 \pm 801.02$	$1.53e + 03 \pm 783.51$
1%	417.60 ± 166.99	647.58 ± 250.87	588.70 ± 206.50	588.65 ± 250.23
10%	404.50 ± 163.29	578.44 ± 155.51	545.88 ± 207.29	577.39 ± 279.99
100%	392.68 ± 150.13	588.08 ± 204.18	477.86 ± 177.34	484.74 ± 100.42

Dataset Size	CPN	MAML	PTS	RND
0%	0.31 ± 0.11	0.18 ± 0.04	0.16 ± 0.02	$0.16 \pm 0.00e + 00$
0.1%	0.61 ± 0.15	0.42 ± 0.12	0.44 ± 0.16	0.48 ± 0.12
1%	0.71 ± 0.07	0.63 ± 0.09	0.65 ± 0.08	0.66 ± 0.08
10%	0.72 ± 0.08	0.64 ± 0.06	0.66 ± 0.08	0.66 ± 0.11
100%	0.73 ± 0.07	0.64 ± 0.08	0.69 ± 0.07	0.68 ± 0.05

Figure 23: Quantitative comparison of end-to-end results produced by various initialization methods on color quantization with a palette size of 15 colors. **(Top)** The average mean squared error (MSE) of the image produced by each initialization method compared to the image produced by a ground-truth implementation of the `kmeans` kernel (lower is better). **(Bottom)** The average structural similarity index measure (SSIM) of the image produced by each initialization method compared to the image produced by a ground-truth implementation of the `kmeans` kernel (higher is better).

Statistic	CPN	MAML	PTS
0th	0.03×	0.06×	0.03×
25th	1.16×	0.85×	0.61×
50th	3.43×	1.19×	1.03×
75th	23.96×	1.68×	1.56×
100th	$8.27 \cdot 10^3$×	26.54×	49.39×
MPI	18th	36th	48th
GM	7.28×	1.16×	0.93×

Figure 24: Geometric mean and percentile improvements to training time over random initialization on a sample of 1,000 EXESTACKCPN test programs. MPI is the minimum percentile at which an initialization method improves over random initialization.

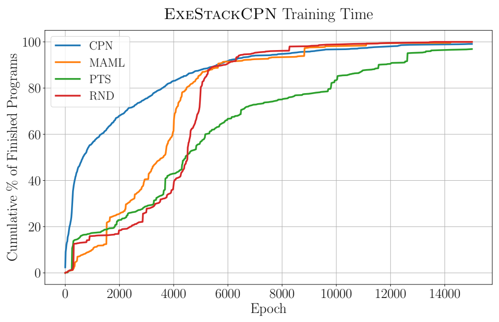

Figure 25: Epoch vs. percentage of EXESTACKCPN programs that each initialization method finished at that epoch.

discard these results before computing the geometric mean.

There are a few subtleties in this methodology. First, note that random initialization does not always have a finish epoch of 5,000, because the target error set after 5,000 epochs of training may have already been achieved earlier in training. Also, since the timeout epoch (15,000) is 3× the baseline finish epoch (5,000), the worst case slowdown for each initialization method is $\frac{1}{3}$×.

Visualizing Results. Since we evaluate on many programs in EXESTACKCPN, we plot the number of finished programs as a function of the number of epochs for each initialization method. For each program and initialization method, we calculate the finish epoch for that program as the average finish epoch over all instances of the initialization method and all trials for that instance.

L.0.2. RESULTS

The results are summarized in Figures 24and 25 for the sample of EXESTACKCPN test programs and Figures 26 and 27 for ParrotBenchShort.

EXESTACKCPN Test Programs. COMPNETS achieve the best results on average, with a 7.28× improvement over random initialization, whereas MAML and pretrained surrogates achieve 1.16× and 0.93× improvements, respectively. COMPNETS improve over random initialization in as low as the 18th perecentile, whereas MAML and pretrained surrogates improve over random initialization after the 36th and 48th percentile, respectively.

Until the ≈ 5,000th epoch, COMPNETS finish training on strictly more programs than all other initialization methods. At the 5,000th epoch, COMPNETS finish training for ≈ 90% of programs. For the remaining 10% of programs, random initialization and MAML begin to overtake COMPNETS, at epochs ≈ 6,250 and ≈ 9,000, respectively.

Statistic	CPN	MAML	PTS
0th	0.39×	0.38×	0.42×
25th	0.54×	0.63×	0.57×
50th	1.01×	0.96×	0.83×
75th	108.21×	1.07×	7.91×
100th	849.78×	25.66×	278.11×
MPI	50th	54th	60th
GM	4.31×	1.07×	2.35×

Figure 26: Geometric mean (GM) training time improvements over random initialization (MPI) on PARROTBENCHSHORT. The percentiles from 0th to 100th are the minimum percentile at which an initialization method improves over random initialization.

Program	CPN	MAML	PTS
`fft`	1.43×	0.83×	0.80×
`invk2j`	0.49×	0.65×	0.56×
`kmeans`	674.47×	2.15×	86.87×
`sobel`	0.74×	1.14×	0.79×

Figure 27: Geometric mean training time improvements over random initialization take over all of PARROTBENCHSHORT.

PARROTBENCHSHORT Programs. COMPNETS achieve the best results on average, with a 4.31× improvement over random initialization, whereas MAML and pretrained surrogates achieve 1.07× and 2.35× improvements, respectively. COMPNETS improve over random initialization after the 50th perecentile, MAML improves over random initialization after the 54th percentile, and pretrained surrogates improve over random initialization after the 48th percentile.

COMPNETS range between improvements of 0.49× on `invk2j` to 674× on `kmeans`. The variance between other techniques is less pronounced, with MAML varying between $0.65\times$ on `invk2j` and $2.15\times$ on `kmeans`, and pretrained surrogates varying between $0.56\times$ on `invk2j` and $87\times$ on `kmeans`. Since all results present slowdowns on `invk2j` and speedups on `kmeans`, it is possible `ExeStackCPN` does not include similar computations to `invk2j` but does include similar computations to `kmeans`. We use an extensive decontamination methodology (see Appendix E.1), so we conclude these similarities are abstract in nature.

Since COMPNETS improve training time over random initialization on both EXESTACKCPN and PARROTBENCHSHORT, we answer yes to RQ 2.

Additional Data. We present the initial train losses, initial test lossses, and target test losses for both EXESTACKCPN (Figure 28) and PARROTBENCHSHORT (Figures 29, 30, and 31). We also present the average finish epoch (Figure 32) for each initialization method and the number of timeouts (Figure 33) on PARROTBENCHSHORT programs.

M. Acceptable Surrogate Error

In this section, we show that, in the context of our evaluation, the error incurred from using neural surrogates is satisfactory for downstream applications. We first show that the surrogates of Esmaeilzadeh et al. (2012a) achieve acceptable end-to-end error on PARROTBENCHSHORT and that our surrogates achieve commensurate error with their surrogates. Then, we explain that the error incurred from datatype mismatches alone is negligible for PARROTBENCHSHORT.

M.1. End-to-End Error

Esmaeilzadeh et al. calculate end-to-end error for the benchmarks we consider from PARROTBENCH as follows:

- **`fft`.** Apply the fast Fourier transform to a sequence of 2,048 values, where the value at the ith index is i, and measure the average relative error between the output of the original `fft` implementation and the approximate `fft` implementation.
- **`invk2j`.** Generate 1,000 pairs of joint angles (θ_1, θ_2), with both angles sampled uniformly at random from $[0, \pi/2]$. Run forward kinematics on these angles, to obtain (x, y) coordinates for the tip of the joint arm. Run inverse kinematics on these (x, y) coordinates, to obtain joint angles $(\tilde{\theta_1}, \tilde{\theta_2})$ that place the tip of the joint arm at (x, y). Measure the average relative error between the joint angles recovered by the original `invk2j` implementation and the approximate `invk2j` implementation.
- **`kmeans`.** Apply one iteration of k-means clustering to each pixel of the image in Figure 16, then set each pixel's color to the color of the closest centroid. Measure the average root mean squared error between the image produced by the original `kmeans` implementation and the approximate `kmeans` implementation.
- **`sobel`.** Convert the image in Figure 16 to grayscale using a weighted average of 30% red, 59% green, and 11% blue. Apply the `sobel` filter to the first row of the image, the first column, and the last row. Measure the average root mean squared error between the image produced by the original `sobel` implementation and the approximate `sobel` implementation.

The end-to-end error of the neural-surrogate-based implementation of each benchmark reported by Esmaeilzadeh et al. is $\leq 7.5\%$ on the subset of PARROTBENCH benchmarks we draw from (see Figure 34). An end-to end quality loss of 10% or more is common in the approximate computing literature (Esmaeilzadeh et al., 2012a;b; Sampson et al., 2011; Baek & Chilimbi, 2010; Misailovic et al., 2010). For example, Park et al. develop neural surrogates of programs for image processing, audio processing, and speech processing, and they collect user feedback on the perceptual quality of the approximate programs (Park et al., 2016). Their results show that, on a majority of the benchmarks they consider, a quality loss of $\geq 10\%$ is deemed acceptable by $\geq 80\%$ of users. The neural surrogates we train achieve commensurate and often lower test error than the surrogates of Esmaeilzadeh et al. (2012a). Thus, the neural surrogates we train achieve an acceptable level of approximation.

M.2. Datatype Mismatch Error

The neural surrogates we compile to and finetune use single-precision data types, but 59% of EXESTACKCPN programs use at least one double-precision datatype and 56% of EXESTACKCPN programs use exclusively double-precision datatypes.

We generate two versions of each PARROTBENCHSHORT program: one using only `float` and one using only `double`. We then generate random double-precision inputs according to the methodology in Section F.2 and execute each version of each program. We report the mean squared error (MSE) between the outputs of the single- and double-precision versions of each program in Figure 34 (Bottom).

Between the `float` and `double` implementations, the largest mean squared error (MSE) we observe is $5.3 \cdot 10^{-4}$ for `invk2j` (0). The neural surrogate approximation error is $5.6 \cdot 10^{-3}$, an order of magnitude larger. The discrepancy is even larger for every other benchmark.

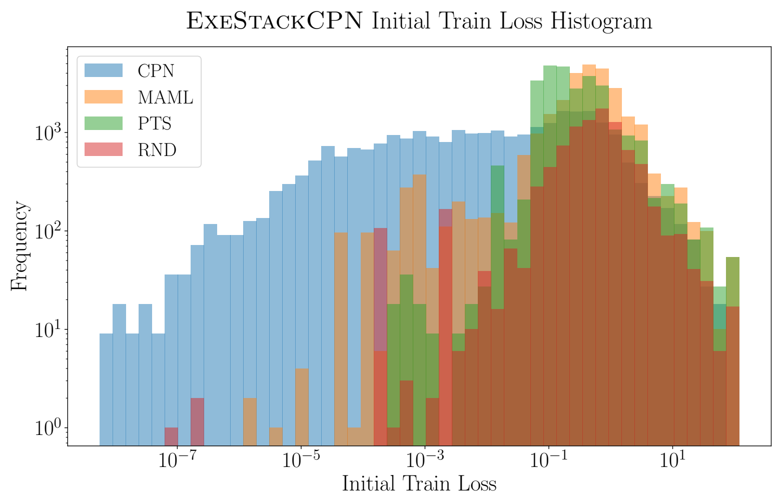

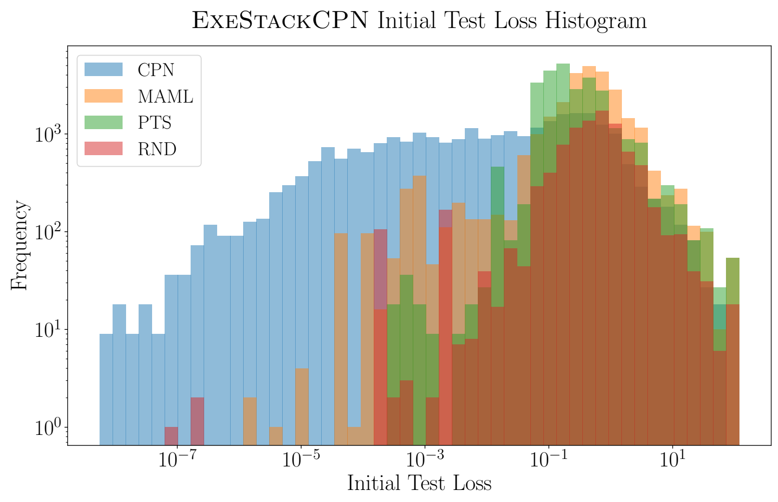

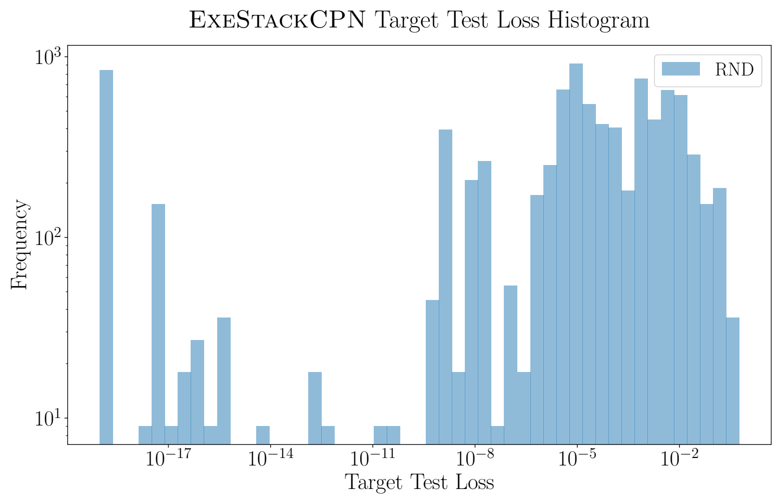

Figure 28: Histogram of initial train losses (top) and initial test losses (bottom) for surrogats produced by each initialization method in the training time evaluation, as well as a histogram of the target test losses set by random initialization after training for 5,000 epochs. Losses are not averaged across instances of initialization methods and trials. Note that both the x and y axes are log-scale.

Program	CPN (0)	CPN (1)	CPN (2)	CPN
`fft`	$0.48 \pm 1.81 \cdot 10^{-6}$	$0.43 \pm 8.51 \cdot 10^{-6}$	$2.94 \pm 6.80 \cdot 10^{-5}$	1.28 ± 1.20
`invk2j`	$1.14 \pm 5.67 \cdot 10^{-4}$	$1.90 \pm 8.89 \cdot 10^{-4}$	$2.54 \pm 1.52 \cdot 10^{-3}$	1.86 ± 0.58
`kmeans`	$0.12 \pm 1.44 \cdot 10^{-5}$	$0.09 \pm 1.33 \cdot 10^{-5}$	$0.08 \pm 1.20 \cdot 10^{-5}$	0.10 ± 0.02
`sobel`	$0.09 \pm 3.62 \cdot 10^{-4}$	$0.13 \pm 4.21 \cdot 10^{-4}$	$0.17 \pm 3.72 \cdot 10^{-4}$	0.13 ± 0.03

Program	MAML (0)	MAML (1)	MAML (2)	MAML
`fft`	0.57 ± 0.18	0.59 ± 0.19	0.53 ± 0.14	0.56 ± 0.16
`invk2j`	2.08 ± 0.64	2.07 ± 0.59	2.02 ± 0.56	2.06 ± 0.58
`kmeans`	0.76 ± 0.46	0.64 ± 0.38	0.79 ± 0.52	0.73 ± 0.44
`sobel`	0.24 ± 0.16	0.18 ± 0.12	0.25 ± 0.22	0.22 ± 0.17

Program	PTS (0)	PTS (1)	PTS (2)	PTS
`fft`	0.83 ± 0.07	0.84 ± 0.07	0.84 ± 0.07	0.84 ± 0.07
`invk2j`	2.11 ± 0.57	2.10 ± 0.56	2.12 ± 0.59	2.11 ± 0.55
`kmeans`	$0.10 \pm 1.92 \cdot 10^{-5}$	$0.10 \pm 1.88 \cdot 10^{-5}$	$0.10 \pm 1.87 \cdot 10^{-5}$	$0.10 \pm 1.34 \cdot 10^{-3}$
`sobel`	$0.18 \pm 4.37 \cdot 10^{-4}$	$0.19 \pm 4.40 \cdot 10^{-4}$	$0.19 \pm 4.43 \cdot 10^{-4}$	$0.19 \pm 3.55 \cdot 10^{-3}$

Program	RND
`fft`	0.64 ± 0.35
`invk2j`	2.37 ± 0.80
`kmeans`	0.24 ± 0.25
`sobel`	0.36 ± 0.34

Figure 29: Average initial train loss on PARROTBENCHSHORT for surrogates produced by each initialization method. We include a column for each instance of an initialization method (e.g., “CPN (0)” is only one of the COMPNETs we trained) as well as a column that averages over each instance (e.g., “CPN” is an average over all COMPNETs we trained).

Program	CPN (0)	CPN (1)	CPN (2)	CPN
`fft`	0.48 ± 0.00	0.42 ± 0.00	2.92 ± 0.00	1.27 ± 1.18
`invk2j`	1.14 ± 0.00	1.89 ± 0.00	2.51 ± 0.00	1.84 ± 0.57
`kmeans`	0.06 ± 0.00	0.06 ± 0.00	0.05 ± 0.00	0.06 ± 0.01
`sobel`	0.09 ± 0.00	0.13 ± 0.00	0.17 ± 0.00	0.13 ± 0.03

Program	MAML (0)	MAML (1)	MAML (2)	MAML
`fft`	0.57 ± 0.18	0.59 ± 0.19	0.53 ± 0.14	0.56 ± 0.17
`invk2j`	2.07 ± 0.63	2.06 ± 0.59	2.01 ± 0.56	2.05 ± 0.57
`kmeans`	0.71 ± 0.43	0.60 ± 0.37	0.74 ± 0.50	0.68 ± 0.42
`sobel`	0.24 ± 0.16	0.18 ± 0.12	0.25 ± 0.22	0.22 ± 0.17

Program	PTS (0)	PTS (1)	PTS (2)	PTS
`fft`	0.83 ± 0.07	0.84 ± 0.07	0.85 ± 0.07	0.84 ± 0.07
`invk2j`	2.09 ± 0.57	2.09 ± 0.56	2.11 ± 0.58	2.10 ± 0.55
`kmeans`	0.06 ± 0.00	0.06 ± 0.00	0.06 ± 0.00	$0.06 \pm 7.58 \cdot 10^{-4}$
`sobel`	0.18 ± 0.00	0.19 ± 0.00	0.19 ± 0.00	$0.19 \pm 3.52 \cdot 10^{-3}$

Program	RND
`fft`	0.64 ± 0.36
`invk2j`	2.36 ± 0.80
`kmeans`	0.21 ± 0.23
`sobel`	0.36 ± 0.34

Figure 30: Average initial test loss on PARROTBENCHSHORT for surrogates produced by each initialization method. We include a column for each instance of an initialization method (e.g., "CPN (0)" is only one of the COMPNETs we trained) as well as a column that averages over each instance (e.g., "CPN" is an average over all COMPNETs we trained).

Program	RND
`fft`	$3.96 \cdot 10^{-6}$
`invk2j`	$2.83 \cdot 10^{-3}$
`kmeans`	0.01
`sobel`	$4.16 \cdot 10^{-4}$

Figure 31: Target test loss for each PARROTBENCHSHORT program, set by training randomly initialized surrogates for $5{,}000$ epochs over 9 trials and using the average final test loss.

Program	CPN-R Z/Z (Clone) (0)	CPN-R Z/Z (Clone) (1)	CPN-R Z/Z (Clone) (2)	CPN-R Z/Z (Clone)
`fft`	379.7 ± 31.5	262.0 ± 15.9	1140.7 ± 40.3	594.1 ± 398.0
`invk2j`	15000.0 ± 0.0	9200.7 ± 885.0	12581.3 ± 1956.4	12260.7 ± 2700.6
`kmeans`	12.0 ± 1.5	6.0 ± 0.0	6.0 ± 0.0	8.0 ± 3.0
`sobel`	11316.7 ± 2774.9	10637.0 ± 2332.6	4232.3 ± 2168.6	8728.7 ± 4008.5

Program	MAML-Z Z/Z (Reinit) (0)	MAML-Z Z/Z (Reinit) (1)	MAML-Z Z/Z (Reinit) (2)	MAML-Z Z/Z (Reinit)
`fft`	649.3 ± 469.7	824.0 ± 527.4	1069.0 ± 1047.5	847.4 ± 722.4
`invk2j`	9837.3 ± 5124.5	5327.7 ± 4358.9	13949.0 ± 3153.0	9704.7 ± 5464.3
`kmeans`	198.7 ± 192.1	13338.7 ± 4984.0	5018.0 ± 7486.5	6185.1 ± 7449.2
`sobel`	5695.7 ± 3764.1	6572.7 ± 5221.4	3668.3 ± 2193.8	5312.2 ± 3970.6

Program	PTS (0)	PTS (1)	PTS (2)	PTS
`fft`	459.3 ± 241.2	1384.7 ± 1098.1	1024.3 ± 1087.0	956.1 ± 950.3
`invk2j`	13794.3 ± 3345.0	12470.3 ± 5072.0	6632.7 ± 5282.7	10965.8 ± 5477.0
`kmeans`	188.0 ± 36.3	58.7 ± 42.3	18.3 ± 1.0	88.3 ± 80.0
`sobel`	9964.0 ± 4035.9	5436.7 ± 120.1	7555.7 ± 485.2	7652.1 ± 2939.6

Program	RND
`fft`	693.0 ± 689.0
`invk2j`	5835.7 ± 5133.0
`kmeans`	5098.7 ± 7429.2
`sobel`	5881.0 ± 3900.7

Figure 32: Average epoch at which each initialization method achieves the target test loss for the training time evaluation on PARROTBENCHSHORT. We include a column for each instance of an initialization method (e.g., "CPN (0)" is only one of the COMPNETS we trained) as well as a column that averages over each instance (e.g., "CPN" is an average over all COMPNETS we trained).

Program	CPN (0)	CPN (1)	CPN (2)	CPN
`fft`	0/9	0/9	0/9	0/27
`invk2j`	9/9	0/9	3/9	12/27
`kmeans`	0/9	0/9	0/9	0/27
`sobel`	0/9	0/9	0/9	0/27

Program	MAML (0)	MAML (1)	MAML (2)	MAML
`fft`	0/9	0/9	0/9	0/27
`invk2j`	4/9	1/9	8/9	13/27
`kmeans`	0/9	8/9	3/9	11/27
`sobel`	1/9	2/9	0/9	3/27

Program	PTS (0)	PTS (1)	PTS (2)	PTS
`fft`	0/9	0/9	0/9	0/27
`invk2j`	7/9	7/9	1/9	15/27
`kmeans`	0/9	0/9	0/9	0/27
`sobel`	3/9	0/9	0/9	3/27

Program	RND
`fft`	0/9
`invk2j`	0/9
`kmeans`	3/9
`sobel`	1/9

Figure 33: Number of trials where each initialization method does not achieve the target test loss after training for 15,000 epochs during the training time evaluation on PARROTBENCHSHORT. We include a column for each instance of an initialization method (e.g., "CPN (0)" is only one of the COMPNETs we trained) as well as a column that sums over each instance (e.g., "CPN" is a sum over all COMPNETs we trained).

Benchmark	CPN	MAML	PTS	RND	PRT	E2E Error
`fft`	$4.3 \cdot 10^{-6}$	$3.1 \cdot 10^{-6}$	$5.3 \cdot 10^{-6}$	$3.2 \cdot 10^{-6}$	$2 \cdot 10^{-5}$	7.22%
`invk2j`	$3.3 \cdot 10^{-3}$	$3.3 \cdot 10^{-3}$	$3.4 \cdot 10^{-3}$	$3.1 \cdot 10^{-3}$	$5.6 \cdot 10^{-3}$	7.50%
`kmeans`	$3.4 \cdot 10^{-3}$	$1.3 \cdot 10^{-2}$	$5.2 \cdot 10^{-3}$	$8.3 \cdot 10^{-3}$	$1.7 \cdot 10^{-3}$	6.18%
`sobel`	$5.4 \cdot 10^{-4}$	$4.5 \cdot 10^{-4}$	$6.3 \cdot 10^{-4}$	$4.2 \cdot 10^{-4}$	$2.3 \cdot 10^{-3}$	3.44%

Benchmark	`float` vs. `double` MSE
`fft` (0)	$1.2 \cdot 10^{-14}$
`fft` (1)	$1.1 \cdot 10^{-14}$
`invk2j` (0)	$5.3 \cdot 10^{-4}$
`invk2j` (1)	$7.6 \cdot 10^{-12}$
`kmeans`	0.0
`sobel`	$6.51 \cdot 10^{-8}$

Figure 34: **(Top)** Mean squared error (MSE) on PARROTBENCHSHORT test set for each initialization method in our evaluation, MSE of the neural surrogates Esmaeilzadeh et al. (2012a) train, and the end-to-end error achieved by the surrogates of Esmaeilzadeh et al (PRT). **(Bottom)** MSE between PARROTBENCHSHORT implementations that solely use the `float` datatype and implementations that solely use the `double` datatype. To calculate MSE, each program is evaluated on all inputs from the train and test set of PARROTBENCHSHORT, and MSE is computed using the programs' outputs.

N. Padding Inputs For Variable-Input Support

As explained in Section 3, the COMPNET architecture outputs a fixed-size weight vector. To develop a variable-input neural surrogate compiler, we chose a vector size with as many parameters as the architecture with the largest number of inputs we wish to support. However, when one compiles a program with fewer inputs than the target architecture, one must supply values to the excess inputs or remove these neurons from the architecture. Supplying zeroes for the excess inputs is mathematically equivalent to removing the neurons, so we characterize each strategy purely in terms of data. Furthermore, there are three phases in which data is supplied to the system: neural surrogate compiler training, compiled surrogate finetuning, and compiled surrogate evaluation. Thus, we categorize the strategies we consider by the type of data the neural surrogate compiler is trained on, the type of data the compiled surrogates are finetuned on, and the type of data the compiled surrogates are evaluated on.

Methodology. There are two types of data we considered: random padding and zero padding. With random padding, any excess inputs are supplied with values from the same distribution as the primary inputs. With zero padding, any excess inputs are supplied with zeroes. We considered most permutations of random and zero padding for the three phases of training described in the previous paragraph. Notably, however, we did not consider the family of strategies where one finetunes on zero-padded inputs and evaluates on random-padded inputs because it seemed unlikely that adding a new source of noise at inference time would lead to any improvement.

To decide which strategy to use for each initialization method, we performed the PARROTBENCHSHORT data efficiency evaluation of Section 5.2 with a set of padding strategies applied to each initialization method. For each initialization method, we chose the strategy that achieved the greatest overall test loss improvement over random initialization. Note that these experiments were performed prior to adding variable-output support, so we split the `fft` and `invk2j` benchmarks in PARROTBENCHSHORT into multiple programs—one for each output.

Results. We present the results in separate figures for random initialization (Figure 35), pretrained surrogates trained on random-padded and zero-padded inputs (Figures 36 and 37), MAML initializations trained on random-padded and zero-padded inputs (Figures 38 and 39), and COMPNETS trained on random-padded and zero-padded inputs (Figures 40 and 41).

Random initialization sees performance degradation with every padding strategy. One explanation for this degradation is that the baseline is random initialization with an architecture that has exactly as many inputs as needed, whereas each of the padding strategies operates on the largest encompassing architecture. Since the magnitude of weights in the He initialization is inversely proportional to the fan-in and fan-out of a neuron (He et al., 2015), the magnitude of weights in the first layer of the network will be smaller, potentially slowing convergence.

Surrogates that are pretrained on random-padded inputs perform approximately as well as surrogates pretrained on zero-padded inputs for all finetuning and evaluation variants. Among the finetuning and evaluation variants, finetuning and evaluating on zero-padded inputs performs the best. The best configuration by a small margin is pretraining on random-padded inputs and finetuning and evaluating on zero-padded inputs; this configuration achieves a geometric mean test loss improvement of $1.13\times$.

Across all finetuning and evaluation modes, MAML initializations trained on zero-padded inputs outperform MAML initializations trained on random-padded inputs. When MAML initializations are trained on zero-padded inputs, finetuning and evaluating on zero-padded inputs leads to the greatest geometric mean test loss improvement of $1.29\times$ over random initialization.

Across all finetuning and evaluation modes, COMPNET initializations trained on random-padded inputs outperform COMPNET initializations trained on zero-padded inputs. When COMPNET initializations are trained on random-padded inputs, finetuning and evaluating on zero-padded inputs leads to the greatest geometric mean test loss improvement of $1.96\times$ over random initialization.

Conclusion. In light of these results, we make the following decisions. We choose standard random initialization over any of the padded variants; we choose pretrained surrogates that are pretrained on random-padded inputs and finetuned and evaluated on zero-padded inputs; we choose MAML initializations that are trained, finetuned, and evaluated on zero-padded inputs; and we choose COMPNETS that are trained on random-padded inputs and the surrogates they produce are finetuned and evaluated on zero-padded inputs.

The reason why some initialization methods perform better when training on random-padded inputs and others perform better when training on zero-padded inputs is unclear and deserves further study.

O. Strategies for Variable-Output Program Support

Recall, all programs in EXESTACK have a single output (Section 4). However, the `fft` and `invk2j` benchmarks in PARROTBENCHSHORT have multiple outputs. In this

Program	RND	RND FT-R EV-R	RND FT-R EV-Z	RND FT-Z EV-Z
`fft` (0)	$1.00\times$	$0.02\times$	$0.02\times$	$0.19\times$
`fft` (1)	$1.00\times$	$0.18\times$	$0.23\times$	$1.06\times$
`invk2j` (0)	$1.00\times$	$0.45\times$	$0.53\times$	$1.00\times$
`invk2j` (1)	$1.00\times$	$0.31\times$	$0.32\times$	$0.82\times$
`kmeans`	$1.00\times$	$0.64\times$	$0.65\times$	$0.83\times$
`sobel`	$1.00\times$	$1.00\times$	$1.00\times$	$1.00\times$

Dataset Size	RND	RND FT-R EV-R	RND FT-R EV-Z	RND FT-Z EV-Z
0%	$1.00\times$	$0.80\times$	$0.80\times$	$0.80\times$
0.1%	$1.00\times$	$0.05\times$	$0.08\times$	$0.51\times$
1%	$1.00\times$	$0.10\times$	$0.10\times$	$0.39\times$
10%	$1.00\times$	$0.22\times$	$0.23\times$	$1.01\times$
100%	$1.00\times$	$1.22\times$	$1.29\times$	$1.18\times$

Statistic	RND	RND FT-R EV-R	RND FT-R EV-Z	RND FT-Z EV-Z
0th	$1.00\times$	$4.46 \cdot 10^{-4}\times$	$6.03 \cdot 10^{-4}\times$	$0.01\times$
25th	$1.00\times$	$0.27\times$	$0.30\times$	$0.92\times$
50th	$1.00\times$	$0.83\times$	$0.86\times$	$1.00\times$
75th	$1.00\times$	$1.00\times$	$1.00\times$	$1.09\times$
100th	$1.00\times$	$5.64\times$	$6.48\times$	$1.66\times$
MPI	0th	68th	63rd	50th
GM	$1.00\times$	$0.26\times$	$0.28\times$	$0.72\times$

Figure 35: Data efficiency results for PARROTBENCHSHORT programs using variants of random initialization. FT-R and FT-Z mean the surrogate initialization was finetuned using random-padded and zero-padded inputs, respectively. EV-R and EV-Z mean the surrogate initialization was evaluated using random-padded and zero-padded inputs, respectively.

Program	PTS-R FT-R EV-R	PTS-R FT-R EV-Z	PTS-R FT-Z EV-Z
`fft` (0)	$0.06\times$	$0.06\times$	$1.53\times$
`fft` (1)	$0.17\times$	$0.19\times$	$0.76\times$
`invk2j` (0)	$0.50\times$	$0.59\times$	$1.18\times$
`invk2j` (1)	$0.28\times$	$0.29\times$	$0.77\times$
`kmeans`	$1.77\times$	$1.80\times$	$2.28\times$
`sobel`	$0.85\times$	$0.85\times$	$0.85\times$

Dataset Size	PTS-R FT-R EV-R	PTS-R FT-R EV-Z	PTS-R FT-Z EV-Z
0%	$1.38\times$	$1.38\times$	$1.38\times$
0.1%	$0.05\times$	$0.06\times$	$1.26\times$
1%	$0.11\times$	$0.12\times$	$1.03\times$
10%	$0.60\times$	$0.62\times$	$0.94\times$
100%	$1.33\times$	$1.45\times$	$1.07\times$

Statistic	PTS-R FT-R EV-R	PTS-R FT-R EV-Z	PTS-R FT-Z EV-Z
0th	$3.50 \cdot 10^{-4}\times$	$4.76 \cdot 10^{-4}\times$	$0.15\times$
25th	$0.26\times$	$0.35\times$	$0.75\times$
50th	$0.73\times$	$0.77\times$	$1.07\times$
75th	$1.38\times$	$1.39\times$	$1.65\times$
100th	$28.05\times$	$28.24\times$	$28.03\times$
MPI	66th	65th	47th
GM	$0.36\times$	$0.39\times$	$1.13\times$

Figure 36: Data efficiency results for ParrotBenchShort programs using pretrained surrogates trained with random-padded inputs. FT-R and FT-Z mean the surrogate initialization was finetuned using random-padded and zero-padded inputs, respectively. EV-R and EV-Z mean the surrogate initialization was evaluated using random-padded and zero-padded inputs, respectively.

Program	PTS-Z FT-R EV-R	PTS-Z FT-R EV-Z	PTS-Z FT-Z EV-Z
`fft` (0)	$0.06\times$	$0.06\times$	$0.95\times$
`fft` (1)	$0.24\times$	$0.33\times$	$1.04\times$
`invk2j` (0)	$0.53\times$	$0.62\times$	$1.25\times$
`invk2j` (1)	$0.35\times$	$0.37\times$	$1.08\times$
`kmeans`	$0.95\times$	$0.93\times$	$1.31\times$
`sobel`	$1.07\times$	$1.07\times$	$1.07\times$

Dataset Size	PTS-Z FT-R EV-R	PTS-Z FT-R EV-Z	PTS-Z FT-Z EV-Z
0%	$1.58\times$	$1.58\times$	$1.58\times$
0.1%	$0.06\times$	$0.09\times$	$1.17\times$
1%	$0.10\times$	$0.10\times$	$1.09\times$
10%	$0.80\times$	$0.84\times$	$1.12\times$
100%	$0.91\times$	$0.96\times$	$0.74\times$

Statistic	PTS-Z FT-R EV-R	PTS-Z FT-R EV-Z	PTS-Z FT-Z EV-Z
0th	$5.52 \cdot 10^{-4}\times$	$6.16 \cdot 10^{-4}\times$	$0.07\times$
25th	$0.37\times$	$0.47\times$	$0.87\times$
50th	$0.84\times$	$0.84\times$	$1.10\times$
75th	$1.13\times$	$1.19\times$	$1.41\times$
100th	$10.94\times$	$12.86\times$	$7.41\times$
MPI	66th	65th	41st
GM	$0.37\times$	$0.41\times$	$1.11\times$

Figure 37: Data efficiency results for ParrotBenchShort programs using pretrained surrogates trained with zero-padded inputs. FT-R and FT-Z mean the surrogate initialization was finetuned using random-padded and zero-padded inputs, respectively. EV-R and EV-Z mean the surrogate initialization was evaluated using random-padded and zero-padded inputs, respectively.

Program	MAML-R FT-R EV-R	MAML-R FT-R EV-Z	MAML-R FT-Z EV-Z
`fft` (0)	$0.06\times$	$0.07\times$	$1.30\times$
`fft` (1)	$0.32\times$	$0.45\times$	$1.11\times$
`invk2j` (0)	$0.39\times$	$0.48\times$	$0.82\times$
`invk2j` (1)	$0.64\times$	$0.75\times$	$1.13\times$
`kmeans`	$0.63\times$	$0.65\times$	$0.65\times$
`sobel`	$0.44\times$	$0.44\times$	$0.44\times$

Dataset Size	MAML-R FT-R EV-R	MAML-R FT-R EV-Z	MAML-R FT-Z EV-Z
0%	$0.97\times$	$0.97\times$	$0.97\times$
0.1%	$0.06\times$	$0.08\times$	$1.12\times$
1%	$0.12\times$	$0.15\times$	$0.82\times$
10%	$0.51\times$	$0.54\times$	$0.56\times$
100%	$1.11\times$	$1.33\times$	$0.90\times$

Statistic	MAML-R FT-R EV-R	MAML-R FT-R EV-Z	MAML-R FT-Z EV-Z
0th	$7.16 \cdot 10^{-4}\times$	$7.54 \cdot 10^{-4}\times$	$0.07\times$
25th	$0.27\times$	$0.32\times$	$0.52\times$
50th	$0.54\times$	$0.58\times$	$0.87\times$
75th	$0.95\times$	$0.99\times$	$1.39\times$
100th	$12.03\times$	$16.94\times$	$15.18\times$
MPI	79th	76th	65th
GM	$0.33\times$	$0.39\times$	$0.85\times$

Figure 38: Data efficiency results for PARROTBENCHSHORT programs using MAML initializations trained with random-padded inputs. FT-R and FT-Z mean the surrogate initialization was finetuned using random-padded and zero-padded inputs, respectively. EV-R and EV-Z mean the surrogate initialization was evaluated using random-padded and zero-padded inputs, respectively.

Program	MAML-Z FT-R EV-R	MAML-Z FT-R EV-Z	MAML-Z FT-Z EV-Z
`fft` (0)	$0.18\times$	$0.21\times$	$2.85\times$
`fft` (1)	$0.54\times$	$0.69\times$	$1.16\times$
`invk2j` (0)	$0.62\times$	$0.77\times$	$1.35\times$
`invk2j` (1)	$0.50\times$	$0.56\times$	$1.11\times$
`kmeans`	$0.88\times$	$0.91\times$	$1.04\times$
`sobel`	$0.89\times$	$0.89\times$	$0.89\times$

Dataset Size	MAML-Z FT-R EV-R	MAML-Z FT-R EV-Z	MAML-Z FT-Z EV-Z
0%	$1.35\times$	$1.34\times$	$1.34\times$
0.1%	$0.06\times$	$0.08\times$	$1.40\times$
1%	$0.14\times$	$0.17\times$	$1.38\times$
10%	$1.34\times$	$1.44\times$	$1.16\times$
100%	$2.60\times$	$2.89\times$	$1.19\times$

Statistic	MAML-Z FT-R EV-R	MAML-Z FT-R EV-Z	MAML-Z FT-Z EV-Z
0th	$7.14 \cdot 10^{-4}\times$	$1.08 \cdot 10^{-3}\times$	$0.29\times$
25th	$0.41\times$	$0.46\times$	$0.86\times$
50th	$0.88\times$	$0.91\times$	$1.10\times$
75th	$1.42\times$	$1.43\times$	$1.50\times$
100th	$57.67\times$	$76.44\times$	$13.85\times$
MPI	56th	55th	39th
GM	$0.53\times$	$0.61\times$	$1.29\times$

Figure 39: Data efficiency results for PARROTBENCHSHORT programs using MAML initializations trained with zero-padded inputs. FT-R and FT-Z mean the surrogate initialization was finetuned using random-padded and zero-padded inputs, respectively. EV-R and EV-Z mean the surrogate initialization was evaluated using random-padded and zero-padded inputs, respectively.

Program	CPN-R FT-R EV-R	CPN-R FT-R EV-Z	CPN-R FT-Z EV-Z
`fft` (0)	$0.88\times$	$0.99\times$	$7.18\times$
`fft` (1)	$0.48\times$	$0.73\times$	$1.17\times$
`invk2j` (0)	$0.56\times$	$0.73\times$	$1.09\times$
`invk2j` (1)	$0.55\times$	$0.62\times$	$1.04\times$
`kmeans`	$4.12\times$	$4.26\times$	$5.22\times$
`sobel`	$1.14\times$	$1.14\times$	$1.14\times$

Dataset Size	CPN-R FT-R EV-R	CPN-R FT-R EV-Z	CPN-R FT-Z EV-Z
0%	$1.42\times$	$1.42\times$	$1.42\times$
0.1%	$0.09\times$	$0.14\times$	$2.33\times$
1%	$1.11\times$	$1.44\times$	$2.56\times$
10%	$1.89\times$	$1.99\times$	$2.18\times$
100%	$2.42\times$	$2.57\times$	$1.57\times$

Statistic	CPN-R FT-R EV-R	CPN-R FT-R EV-Z	CPN-R FT-Z EV-Z
0th	$1.18 \cdot 10^{-3}\times$	$1.47 \cdot 10^{-3}\times$	$0.19\times$
25th	$0.49\times$	$0.60\times$	$0.86\times$
50th	$0.99\times$	$1.01\times$	$1.22\times$
75th	$2.17\times$	$2.20\times$	$2.31\times$
100th	$171.49\times$	$191.02\times$	$1478.96\times$
MPI	51st	48th	35th
GM	$0.92\times$	$1.08\times$	$1.96\times$

Figure 40: Data efficiency results for PARROTBENCHSHORT programs using COMPNETs trained on random-padded inputs. FT-R and FT-Z mean the surrogate initialization was finetuned using random-padded and zero-padded inputs, respectively. EV-R and EV-Z mean the surrogate initialization was evaluated using random-padded and zero-padded inputs, respectively.

Program	CPN-Z FT-R EV-R	CPN-Z FT-R EV-Z	CPN-Z FT-Z EV-Z
`fft` (0)	$0.02\times$	$0.02\times$	$0.58\times$
`fft` (1)	$0.24\times$	$0.28\times$	$1.06\times$
`invk2j` (0)	$0.47\times$	$0.61\times$	$1.07\times$
`invk2j` (1)	$0.60\times$	$0.67\times$	$1.62\times$
`kmeans`	$1.45\times$	$1.51\times$	$1.78\times$
`sobel`	$0.91\times$	$0.91\times$	$0.91\times$

Dataset Size	CPN-Z FT-R EV-R	CPN-Z FT-R EV-Z	CPN-Z FT-Z EV-Z
0%	$1.50\times$	$1.51\times$	$1.51\times$
0.1%	$0.05\times$	$0.07\times$	$0.88\times$
1%	$0.10\times$	$0.12\times$	$1.33\times$
10%	$0.40\times$	$0.45\times$	$0.66\times$
100%	$1.65\times$	$1.75\times$	$1.36\times$

Statistic	CPN-Z FT-R EV-R	CPN-Z FT-R EV-Z	CPN-Z FT-Z EV-Z
0th	$3.05 \cdot 10^{-4}\times$	$5.88 \cdot 10^{-4}\times$	$1.52 \cdot 10^{-4}\times$
25th	$0.39\times$	$0.42\times$	$0.77\times$
50th	$0.79\times$	$0.82\times$	$1.14\times$
75th	$1.31\times$	$1.37\times$	$1.60\times$
100th	$70.29\times$	$70.97\times$	$69.18\times$
MPI	63rd	59th	38th
GM	$0.35\times$	$0.39\times$	$1.10\times$

Figure 41: Data efficiency results for PARROTBENCHSHORT programs using COMPNETs trained on zero-padded inputs. FT-R and FT-Z mean the surrogate initialization was finetuned using random-padded and zero-padded inputs, respectively. EV-R and EV-Z mean the surrogate initialization was evaluated using random-padded and zero-padded inputs, respectively.

appendix, we propose and evaluate a set of strategies to adapt initialization methods trained on EXESTACK to support variable-output programs.

Methodology. For each initialization method, we produce a neural surrogate initialization, then apply one of the following strategies:

- **Grow:** Use the initialization produced by the initialization method and extend the final layer with randomly initialized weights to reach the target number of outputs.
- **Reinitialize:** Use the initialization produced by the initialization method but randomly initialize the final layer, sized to match the target number of outputs.
- **Clone:** Use the initialization produced by the initialization method but duplicate the weights for the one active output in the final layer of the initialization, to generate weights for the target number of outputs.

To decide which strategy to use for each initialization method, we performed the PARROTBENCHSHORT data efficiency evaluation of Section 5.2, and we swept over a set of variable-output strategies applied to each initialization method. We used initialization methods that support variable-input programs, using the best strategies from Appendix N. For each initialization method, we choose the strategy that achieves the greatest overall test loss improvement over random initialization.

Results. We present the results for COMPNETS, MAML, and pretrained surrogates in Figures 42, 43, and 44, respectively.

The best-performing strategy for COMPNETS is cloning, with a geometric mean test loss improvement of $1.91\times$, the best-performing strategy for MAML is reinitialization, with a geometric mean test loss improvement of $0.93\times$, and the best-performing strategy for pretrained surrogates is growing, with a geometric mean test loss improvement of $1.05\times$. Note that the `fft` and `invk2j` benchmarks are the only programs where the variable-output strategies are necessary, but we perform each strategy indiscriminately. This indiscriminate application harms performance for the reinitialization strategy on `kmeans` and `sobel` when using COMPNETS and pretrained surrogates. For COMPNETS in particular, if we only applied each strategy where necessary, reinitialization would have outperformed cloning by a small margin.

Conclusion. In light of these results, we make the following decisions. We choose the cloning strategy for COMPNETS, the reinitialization strategy for MAML, and the growing strategy for pretrained surrogates.

Program	CPN-R Z/Z (Grow)	CPN-R Z/Z (Reinit)	CPN-R Z/Z (Clone)
`fft`	0.95×	1.49×	1.47×
`invk2j`	0.86×	1.01×	1.01×
`kmeans`	7.85×	1.77×	7.85×
`sobel`	1.14×	1.12×	1.14×

Dataset Size	CPN-R Z/Z (Grow)	CPN-R Z/Z (Reinit)	CPN-R Z/Z (Clone)
0%	1.86×	0.95×	1.81×
0.1%	1.61×	1.46×	1.98×
1%	1.49×	1.40×	1.77×
10%	2.13×	1.93×	2.38×
100%	1.26×	1.05×	1.68×

Statistic	CPN-R Z/Z (Grow)	CPN-R Z/Z (Reinit)	CPN-R Z/Z (Clone)
0th	0.17×	0.33×	0.22×
25th	0.79×	0.85×	0.88×
50th	1.05×	1.13×	1.23×
75th	1.96×	1.76×	2.96×
100th	106.91×	31.55×	106.91×
MPI	42nd	33rd	36th
GM	1.64×	1.31×	1.91×

Figure 42: Data efficiency results for PARROTBENCHSHORT programs using COMPNETs trained on various variable-output strategies. CPN-R means we train the COMPNETs on random-padded inputs. Z/Z means we finetune and evaluate COMPNET-initialized surrogates on zero-padded inputs (see Appendix N).

Program	MAML-Z Z/Z (Grow)	MAML-Z Z/Z (Reinit)	MAML-Z Z/Z (Clone)
`fft`	$0.65\times$	$0.98\times$	$0.63\times$
`invk2j`	$1.06\times$	$1.07\times$	$0.88\times$
`kmeans`	$0.94\times$	$0.68\times$	$0.94\times$
`sobel`	$0.89\times$	$1.06\times$	$0.89\times$

Dataset Size	MAML-Z Z/Z (Grow)	MAML-Z Z/Z (Reinit)	MAML-Z Z/Z (Clone)
0%	$1.42\times$	$0.90\times$	$1.42\times$
0.1%	$0.92\times$	$0.94\times$	$0.73\times$
1%	$0.73\times$	$0.93\times$	$0.51\times$
10%	$0.88\times$	$1.11\times$	$0.94\times$
100%	$0.60\times$	$0.81\times$	$0.75\times$

Statistic	MAML-Z Z/Z (Grow)	MAML-Z Z/Z (Reinit)	MAML-Z Z/Z (Clone)
0th	$0.15\times$	$0.28\times$	$0.05\times$
25th	$0.64\times$	$0.82\times$	$0.64\times$
50th	$0.92\times$	$0.97\times$	$0.85\times$
75th	$1.14\times$	$1.14\times$	$1.16\times$
100th	$4.01\times$	$1.99\times$	$8.00\times$
MPI	58th	54th	66th
GM	$0.87\times$	$0.93\times$	$0.82\times$

Figure 43: Data efficiency results for PARROTBENCHSHORT programs using MAML initializations trained on various variable-output strategies. MAML-Z means we train the MAML initializations on zero-padded inputs. Z/Z means we finetune and evaluate MAML-initialized surrogates on zero-padded inputs (see Appendix N).

Program	PTS-R Z/Z (Grow)	PTS-R Z/Z (Reinit)	PTS-R Z/Z (Clone)
`fft`	$0.61\times$	$0.88\times$	$0.46\times$
`invk2j`	$1.05\times$	$0.95\times$	$1.12\times$
`kmeans`	$2.24\times$	$0.65\times$	$2.24\times$
`sobel`	$0.85\times$	$0.92\times$	$0.85\times$

Dataset Size	PTS-R Z/Z (Grow)	PTS-R Z/Z (Reinit)	PTS-R Z/Z (Clone)
0%	$1.56\times$	$0.79\times$	$1.65\times$
0.1%	$0.98\times$	$0.93\times$	$0.81\times$
1%	$0.79\times$	$0.87\times$	$0.75\times$
10%	$1.23\times$	$1.00\times$	$1.00\times$
100%	$0.86\times$	$0.67\times$	$0.98\times$

Statistic	PTS-R Z/Z (Grow)	PTS-R Z/Z (Reinit)	PTS-R Z/Z (Clone)
0th	$0.23\times$	$0.22\times$	$0.21\times$
25th	$0.75\times$	$0.77\times$	$0.65\times$
50th	$0.97\times$	$0.93\times$	$0.85\times$
75th	$1.26\times$	$1.04\times$	$1.40\times$
100th	$38.18\times$	$1.86\times$	$38.18\times$
MPI	54th	69th	63rd
GM	$1.05\times$	$0.84\times$	$1.00\times$

Figure 44: Data efficiency results for ParrotBenchShort programs using pretrained initializations trained on various variable-output strategies. PTS-R means we train the pretrained initializations on random-padded inputs. Z/Z means we finetune and evaluate pretrain-initialized surrogates on zero-padded inputs (see Appendix N).